SUSTAINABLE, GREEN, AND CONTINUOUS SYNTHESIS AND CHARACTERIZATION OF PALLADIUM NANORODS

By

VINDULA BASNAYAKE

Bachelor of Science Chemical Engineering

Mississippi State University

Starkville, Mississippi

2019

Submitted to the Faculty of the
Graduate College of the
Oklahoma State University
in partial fulfillment of
the requirements for
the Degree of
MASTER OF SCIENCE
May, 2021

SUSTAINABLE, GREEN, AND CONTINUOUS

SYNTHESIS AND CHARACTERIZATION OF

PALLADIUM NANORODS

Thesis Approved:

Dr. Shohreh Hemmati, PhD

Thesis Adviser

Dr. Josh Ramsey, PhD

Dr. Toby Nelson, PhD

Name: VINDULA BASNAYAKE

Date of Degree: MAY, 2021

Title of Study: SUSTAINABLE, GREEN, AND CONTINUOUS SYNTHESIS AND CHARACTERIZATION OF PALLADIUM NANORODS
Major Field: CHEMICAL ENGINEERING

Abstract: SUSTAINABLE, GREEN, AND CONTINUOUS SYNTHESIS AND CHARACTERIZATION OF PALLADIUM NANORODS

Pd nanorods have demonstrated many useful applications in multiple fields of science and engineering[1]. This has encouraged further investigation into Pd nanorod synthesis in recent years. Current methods of metal nanostructure synthesis are not environmentally friendly or sustainable due to the use of harmful chemicals such as ethylene glycol and energy intensive reactions[2]. This study examines two possible green alternatives for Pd nanorod synthesis that includes the use of both green reducing agents and solvents, or application of rod-shape virus-like-particles (VLPs) as biotemplate. A literature review on Pd nanorod synthesis using aforementioned sustainable methods as well as its application in different fields was conducted.
For first approach, different reducing agents were tried, and ascorbic acid was chosen for further study as a suitable reducing agent for sustainable synthesis of Pd nanorods by reducing a Pd precursor salt. Continuous-flow millifluidic reactors were employed to enhance yield of synthesized Pd nanorods with better size and morphology control. Compartmentalized flow of the reaction solution was achieved by conducting experiment at boiling point of aqueous solvent that led to uniform liquid plugs of the solution being transported by vaporized solvent and contributed to enhanced Pd nanostructure synthesis via better heat transfer and reactant mixing[3]. Parametric study examined the effect of different factors such as reactant concentrations on size and morphology of synthesized Pd nanorods using Transmission Electron Microscopy (TEM). A kinetic study was performed to examine correlation of reduction rate to the formation of desired seeds, and its effect on the yield of Pd nanorods using Ultraviolet-Visible (UV-Vis) spectroscopy.
For second approach, Tobacco Mosaic Virus (TMV) VLPs were used as a rod-shape viral biotemplate for palladium nanorod synthesis in an aqueous solution without addition of external reducing agent. Functional groups present on TMV VLP capsid protein are capable of reducing Pd precursor salt to achieve a coating of mineralized Pd metal. TMV VLPs were obtained through expression in *Escherichia coli (E-coli)* bacterial medium. Pd mineralization on the outer-wall of capsid protein of TMV VLPs was attempted using batch synthesis method.

TABLE OF CONTENTS

Chapter Page

LIST OF TABLES

Table Page

LIST OF FIGURES

Figure Page

CHAPTER I
INTRODUCTION

Special Properties of Pd

Pd (Palladium) is a noble metal with unique characteristics that allow its use for a wide range of modern applications. Pd is the forty-sixth element on the periodic table and is a d-block transition metal with a face centered cubic (fcc) crystal structure[4]. The unique electronic characteristics and crystal structure of Pd demonstrate several desirable properties such as electrical and thermal conductivity, catalytic behavior and paramagnetism. These properties make Pd useful as a catalyst, an important material in the manufacture of electronics, sensors, and data storage devices. Along with other transition metals, Pd has free electrons in the outer energy levels due to poor shielding by d-orbitals. The mobile electrons also result in better thermal conductivity in Pd[5]. Metallic Pd also demonstrates high affinity to adsorption of certain molecules such as hydrogen, which makes it useful for catalyzing certain types of reactions such as hydrogenation. These properties have been utilized in the modern world, with the most widespread application of Pd being automobile catalytic converters[6]. The characteristic capability of Pd to catalyze oxidation reactions is used in oxidizing pollutants such as carbon-monoxide and hydrocarbon gases. Pd is typically supported on substrates and alloyed with less expensive metals due to the extremely high price of Pd. The effort of using minimum possible amounts of Pd is also evident

in catalytic converters because it usually consists of a ceramic substrate coated with a Pd and Pt alloy.

Pd Nanostructures

Application of Pd nanostructures is a more effective approach to conserving the use of a highly priced precious metal such as Pd while exploiting the beneficial properties of the metal to a maximum. Nanostructures have high surface area to volume ratio because this value is inversely proportional to its characteristic dimension. For example, the surface to volume ratio of spherical structures is inversely proportional to their radius. The high surface to volume ratio of nanostructures maximize the metal surface exposed to the environment, therefore can be an alternative to using a substrate to support Pd. This would be useful for applications such as catalysis due to increased surface exposure resulting in more active sites being made available for reacting molecules to adsorb onto. The extremely miniscule scale of the nanostructures would also make them useful in the manufacture of more complex nanoscale devices such as nanoelectronics[1]. Pd nanostructures can also be synthesized in a wide range of shapes ranging from nanosphere and nanocube to nanorod and nanowire[7]. This is advantageous because each of these nanostructures would have their own characteristic application.

Pd Nanorods – A Novel Tool for the Future?

Nanostructures having at least one dimension between 1 and 100 nm are defined as 1-dimensional (1D) nanostructures and include nanowires, nanotubes and nanorods. 1D nanostructures are categorized based on their aspect ratio. The aspect ratio is defined as the ratio between the length of a nanostructure to its width. There is no fixed rule to differentiate nanorods from nanowires; however, 1D structures with aspect ratios of less than 20 are considered to be nanorods, while nanostructures with greater aspect ratios are considered as nanowires[8].

Pd nanorods in particular have been utilized in several applications including catalysis[9], sensors[10] [11], and magnetic devices[12]. Pd nanorods have been used for catalytic applications involving reactions such as coupling reactions[9], oxidation[13], hydrogenation, and reduction reactions[14]. The highly uniform surfaces of Pd nanorods were found to be very conducive to catalytic activity because it promotes easier alignment of reacting molecules on the active sites of the metal. Pd nanorods were found to be more efficient, and demonstrated high levels of recyclability and catalysis compared to others types of nanostructures such as branched nanocrystals[9]. Pd nanorods have also been integrated into sensors in many studies by exploiting their aforementioned catalytic behavior. The sensors were manufactured by incorporating Pd nanorods onto the surface of the sensor. The compound to be detected will be a molecule that would undergo a specific reaction such as oxidation under the catalytic action of Pd. This chemical conversion would generate an electrochemical change that would be measured and used to determine its concentration. Based on the changes in the current with variation in applied potential, the identity of the compound could also be recognized[15]. The characteristic shape of Pd nanorods also gives it special magnetic properties absent in other Pd nanostructures. Based on the results from superconducting quantum interference device (SQUID) magnetometry, Pd nanorods demonstrated supermagnetic and superparamagnetic behavior, which unfolds opportunities for its

application in many novel areas of technology such as high-density energy storage and spintronic devices[12].

Conventional Methods for Pd Nanorod Synthesis and Their Drawbacks

Pd nanostructures such as nanorods are predominantly synthesized in industry by the polyol method, typically in a batch process. Pd nanostructures are synthesized in polyol process by using polyols such as ethylene glycol[16] or ethaloamine[17] acting as both the solvent and reducing agent along with a metal precursor consisting of a Pd salt such as sodium tetrachloropalladate (Na_2PdCl_4[17]) or palladium trifluoroacetate ($(CF_3COO)_2Pd$)[16]. Nanostructure growth needs to take place only along specific facets for the synthesis of characteristic nanostructures such as 1D nanostructures. Therefore, the other facets are capped by adding capping agents such as potassium bromide (KBr)[16]. The surfaces of the resulting nanostructures need to be stabilized to obtain high quality nanostructures, which require the addition of stabilizing agents such as poly(vinyl pyrrolidone) (PVP)[18]. Recently, there have been concerns about the use of polyol solvents due to their toxicity. For example, prolonged human exposure to ethanolamine could lead to liver damage and bronchitis[19], while ingestion of diethylene glycol could lead to death[20]. The polyol process also takes place at relatively high temperatures, which make these reactions energy intensive and less sustainable.[16] Current studies on synthesis of Pd nanorods mostly use batch reactions. Continuous flow reactors are a promising alternative to batch reactions due to several advantages. Continuous flow in the context of chemical reactions is the uninterrupted flow of a reaction solution through a channel such as tubing to facilitate reactant mixing and heat transfer in place of stirring present in a batch reactor. Continuous-flow synthesis has been used to optimize the synthesis of Pd nanostructures because they provide better control over the mixing

of reagents and enhance heat transfer compared to batch reactions[21]. Continuous flow reactors provide the additional benefits of being a safer alternative, with the ability to scale up reactions conveniently into industrial scale. Reactants present in a continuous flow reactor at any moment is lower than the amount present in a batch reactor that is processing the same total amount of solution; therefore, continuous flow reactors are a safer alternative when a dangerous reaction is taking place[22]. Millifluidic reactors have been used in studies over microfluidic reactors, due to the ease of building a millifluidic reactor with materials available in a laboratory[21 23]. Millifluidic reactors also process larger amounts of reagents in a given period compared to microfluidic reactors. This provides sufficient sample size for characterization and analysis which could pose a problem with smaller samples provided by microfluidic reactors. Continuous flow reactors are easier to be scaled up as this process is guided by simple correlations between the different variables effecting fluid mechanics of the reactor[24]. Continuous flow systems also demonstrate some drawbacks, such as the parabolic velocity profile during laminar flow. The drag of the liquid along the reactor walls lead to the formation of a parabolic velocity profile across the channel's cross section[3]. This causes the solution closer to the walls to move slower compared to the solution at the center; therefore, achieving uneven reaction residence time. The reactors used in continuous flow synthesis are also likely to show irreversible fouling caused by the nanostructures attaching to inner walls of the reactor. This can cause the product quality to deteriorate, or result in the channel being clogged after repeated use[25].

The disadvantages of continuous-flow reactors can be avoided using compartmentalized flow of the reaction solution in the channel. This consists of the solution forming a train of individual segments such as droplets, plugs, or slugs immersed in another medium such as a gas or an immiscible liquid. The tiny volume of an individual liquid segment results in better heat transfer and reactant mixing compared to batch reactions; therefore, produces nanostructures of better quality and reproducibility[3]. The droplets and plugs ensure there is no contact between the reactor

walls and the reaction solution that results in uniform reaction residence times and prevents fouling. These novel millifluidic reactors are also more adaptable for in-situ and real-time characterization techniques such as fiber optic spectroscopic techniques, which can provide valuable knowledge and fundamental understanding regarding the synthesis process.[24].

Green Synthesis – A Better Alternative?

More sustainable approaches to Pd nanostructure synthesis have been explored recently to avoid the negative externalities of the polyol process. This typically involves the use of aqueous solutions instead of glycol solvents and using alternative reducing agents. Lower temperatures are also preferable as this would make the reactions less energy intensive thus more sustainable. This study focuses on two different routes for the green synthesis of Pd nanorods. Application of green solvent and reducing agents and biotemplates are investigated as methods for improving Pd nanorod production with the purpose of making them environmentally friendly and economically feasible alternatives to currently available Pd nanorod synthesis processes.

Conventional Pd nanorod synthesis is also greatly dependent on Batch reactions as the primary mode of Nanorod production. Continuous Flow reactions are potentially superior to batch synthesis from an environmental standpoint, due to the increased safety that they afford and more efficient use of reactants and energy in the reaction relative to a batch reaction; thus, conserving natural resources[22 24]. The use of renewable materials like green reducing agents which are typically sourced from plant matter and viral biotemplates extracted from plants or expressed in bacterial media can be considered to be sustainably sourced. Polyols such as ethylene glycol; however, are commonly synthesized from ethylene and other petroleum based non-renewable precursors[26].

Pd Nanorod Synthesis Using Green Solvent and Reducing Agents

Natural extracts are employed as reducing agents to further improve the sustainability of the Pd nanostructure synthesis process[27] [28]. Batch reactions have been successfully used to synthesize Pd nanorods using a wide range of green reducing agents. For instance, various aqueous plant extracts, vitamins and sugars are able to reduce Pd ions in an aqueous solution resulting in nanostructures of various sizes and morphologies[29]. Many of these reactions are also feasible at lower temperatures relative to polyol process; therefore, requiring less energy[30]. Pd nanorods have in the past, also been successfully synthesized in aqueous solution using green reducing agents such as ascorbic acid[29] and riboflavin[31]. There has been a continued attempt to improve the yields of the nanorods being synthesized. The yield of nanorods is defined as the percentage of the synthesized nanorods with respect to all synthesized nanostructures. Continuous-flow reactors, segmented flow reactions, and reaction parameter optimization can be used to achieve this goal. Such reactions could be an environmentally friendly alternative to the currently used polyol process at the industrial level. An investigation on the Pd nanorod synthesis via a kinetic study would better explain the reaction route and mechanism preferable to nanorod synthesis.

Pd Nanorod Synthesis Using Viral Biotemplates

Another alternative is to use a biotemplate to facilitate Pd mineralization[32]. This bypasses the requirement to add an external reducing agent and would be an environmentally friendly method because the biotemplates could be obtained from natural sources. Biotemplates suitable for the synthesis of nanoscale structures include microorganisms such as bacteria and viruses. Viruses are of particular interest due to many functional groups present on the surface of the capsid protein that reduce the Pd precursor resulting in metal deposition on virion's surface. The various

characteristic shapes of these microorganisms may be used to synthesize Pd nanostructures of different shapes such as spherical shape of M13 bacteriophage virus and rod-like shape of Tobacco Mosaic Virus (TMV) and Barely Stripe Mosaic Virus (BSMV). It is resource and time extensive to extract these viruses from natural sources; because, this method needs to raise plants and animals that would be the hosts for these microorganisms. Virus-Like-Particles (VLPs) poses an easier and more efficient route to obtain viral biotemplates as they can be produced in a laboratory via expression in bacterial media such as *Escherichia Coli (E-coli).*

CHAPTER II
REVIEW OF LITERATURE – PD NANOROD SYNTHESIS USING GREEN REDUCING AGENTS

Green Reducing Agents

There are several naturally occurring substances containing organic side chains that are capable of reducing metal ions found in Pd precursor to form Pd atoms and corresponding Pd nanostructures. This capability is due to the presence of functional groups such as carboxyl, hydroxyl, and carbonyl groups in the reducing agent molecules[33]. The most common side chains that are particularly rich in these components are polyol-like side chains, for example polysaccharides and terpenoids[34]. Other less complex side chains such as amides and amines are also capable of reducing Pd ions. In the case of amine, the presence of a nitrogen with an electron lone pair will facilitate this redox reaction[28 35]. Compounds with these side chains commonly occur in many plants. It is possible to obtain these chemicals from plant matter in the form of solvent extracts[36], gums[37], powders[38], and acids[39]. Sometimes, individual chemical components such as vitamins[31] can be separated from the natural extracts. These extracts may then be applied as reducing agents to synthesize Pd nanostructures. Most of these reagents are non-toxic and are even edible. The plants from which they originate can be commercially cultivated; therefore, are renewable source of reagents. Their widespread use would lead to safer and more sustainable synthesis of Pd nanostructures.

Types of Green Reducing Agents

Aqueous Plant Extracts

The various useful organic molecules present in plants capable of reducing Pd precursors can be conveniently obtained in a laboratory environment by various methods including dissolving finely powdered plant matter in water followed by filtration[40], or the plant matter being boiled in water[41]. These aqueous extracts can then be used as reducing agents in the Pd nanostructure synthesis reactions. A wide range of different useful water-soluble molecules can be extracted in the form of aqueous extracts. These include polyphenols in myrobalan fruit[42] and banana peels[27], and amino acids in soybean leaves[43]. These molecules are especially rich in functional groups such as hydroxyl, carboxylic, amine, and carbonyl groups that donate electrons to the Pd cations present in the reaction solution; therefore, causing them to be reduced into metallic Pd. Many of these molecules also contain electron rich phenol rings that could act as electron donors to the reduction of Pd ions. In addition to being suitable reducing agents, these extracts may also contain certain molecules capable of acting as a stabilizer, which is an added benefit in Pd nanostructure synthesis. The most notable among them is cellulose which is very commonly present in various leaf extracts[40 43]. Cellulose is considered to be insoluble in water but in empirical tests, pure cellulose demonstrates some aqueous solubility; therefore, the compound will also be present in the extracts[44]. Cellulose as a polymer that takes part in polymer adsorption during the growth of metal nanostructures to facilitate the stabilization of various facets resulting in nanostructures with uniform surfaces[45]. This is quite similar to the stabilizing behavior of stabilizing polymers such as PVP.

Sugars

Various sugars and sweeteners have demonstrated the ability to reduce metal ions including Pd and synthesize nanoparticles[46 47]. Sugars are readily available to be purchased at low prices, which is a cost-effective source of reactants for the synthesis of Pd nanostructures. As the materials are readily available and no further processing is required, like in the case of aqueous extracts, experiments could be setup with little effort. Sugar molecules contain electron donating functional groups that are capable of facilitating Pd ion reduction. For example, glucose and dextrose contain multiple hydroxyl groups and saccharine contains both sulfone and carbonyl groups[47]. Sugars also have the additional benefit of being soluble in aqueous solution; thus, not requiring any unsustainable solvents for the synthesis process.

Types of Nanostructures Synthesized Using Green Reducing Agents and Solvents Nanoparticles

Spherical nanostructures are the most commonly synthesized nanoparticles. This is due to the fact that no restriction in the growth of a specific facet of the Pd crystal is required therefore resulting in a spherical shape. This means there is no requirement for a capping agent. Agglomeration could be an issue in the synthesis of these nanostructures because this is encouraged by the Ostwald ripening that cause smaller nanoparticles to aggregate. This may be prevented by the use of either external surfactants. However, one advantage of using green reducing agents, like certain plant extracts, is the presence of compounds that both restrict the effect of Ostwald ripening and discourage agglomeration of nanoparticles[42 48]. Due to the spherical shape of the nanostructures, the main characteristic application observed in recent studies have been catalysis.

Very small uniform nanoparticles provide high surface to volume ratio; therefore, spherical Pd nanoparticles could be used as a catalyst to promote certain chemical reactions[27 46]. The high surface to volume ratio of such nanostructures provides maximum exposure of the antimicrobial metal surface to its environment. This can be advantageous in antibacterial applications as demonstrated by many studies[49 50].

1-Dimensional Nanostructures

One-dimensional nanostructure includes nanowires, nanorods, nanotubes, and nanofibers. These nanostructures are fundamental for the production of nanoelectronics as they could be incorporated into the manufacture of nanoscale circuitry[32]. Capping agents such as KBr usually facilitate the synthesis of such nanostructures as they promote the growth of a single facet over the others; thus, resulting in a high aspect ratio of 1D nanostructures[29]. Alternative methods of nanostructure synthesis are also applicable for the production of these nanostructures but within the scope of green synthesis methods the most cited method is to use a biotemplate. Tobacco Mosaic Virus (TMV) and Barley Stripe Mosaic Virus (BSMV) have been used as biotemplates for the synthesis of Pd nanorods[32 51]. In this case, functional groups on the coat proteins (CPs) of these viruses would reduce the Pd ions in solution, and the mineralized metal would attach itself to the surface of the virion. Generally, the 1D nanostructures synthesized via green reducing agents and viral biotemplates have low aspect ratios when compared to more prevalent methods such as the polyol process. Future research in this field could attempt to achieve higher aspect ratios using green reducing agents[29 30 52] .

Other Nanostructures

In addition to nanoparticles and 1D nanostructures, a range of other structures have also been synthesized using green reducing agents. This includes nanoscale bipyramids[52], nanoflowers[53], nanobelts[54], nanotrees[54], nanoplates[54], nanothetrahedrals[55], and nanocubes[29]. Such a wide variety of nanostructures can be synthesized using natural extracts because they contain molecules that act as capping agents that promote or restrict the growth of specific facets that result in desired shapes[54]. Most of these studies concentrated on generic applications of these Pd nanostructures such as catalysis, with little focus on exploiting their characteristic shapes for specific applications. For example, the cubic shape of silver nanocubes has been used to manufacture gas sensing patches[56]. The development of such niche applications for each of these Pd nanostructures may be the objective of future research initiatives. Further research can also be performed to recognize the specific compounds present in the natural extracts that act as the capping agents that facilitate the synthesis of specific types of nanostructures.

Pd Nanorods Synthesized Using Green Reducing Agents and Solvents

Pd nanorods have been synthesized using different green reducing agents in previous studies including ascorbic acid[2], riboflavin[7], and eugenol[57]. These reducing agents are sourced naturally without requiring any industrial reagents. Similar to other 1D structures, the synthesis of nanorods require the promotion of specific facets over the others; therefore, a capping agent such as KBr is typically employed for this purpose. Control over the rates of reduction is also an important fact as reduction rates which occur too rapidly, may cause most of the Pd precursor to be reduced by the time of facet growth, while slower reduction rates are unfavorable to the

formation of seed structures required in the early phase of nanorod development. Reaction parameters such as temperature and reagent concentrations will play a central role in controlling the reduction rates to maximize synthesis of Pd nanorods.

The size and morphology of desired Pd nanostructures are strongly dependent on the formation, type, and structure of the initially formed seeds. During reduction and nucleation steps, Pd precursor is reduced to form metal atoms that will aggregate to form nuclei. When the size of nuclei is small, a twin defect (a single layer of atoms that mirror (111) plane) can be formed or removed from the nuclei based on free energy. After the nuclei have grown bigger than a specific size, the nuclei become single crystal, single twinned, or multiple twinned seed structures, which will subsequently grow into nanocubes, right bipyramids, and fivefold twinned nanorods, respectively as shown by Figure 1. Multiple twinned seeds can also not undergo any further growth and remain as multiple twinned particles (MTPs) structures by enabling {111} facets have more surface coverage at the lowest level of surface energy. Single-crystal seeds may also evolve into nanobars due to the effect of oxidative etching. Oxidative etching is when metal atoms are oxidized back into ions; therefore, oxidative etching is unfavorable to multiple twinned structure synthesis. Seed crystallinity and the ratio of {100} to {111} facet on its surface is important for synthesizing fivefold twinned nanorods. Production of twinned nanostructures depend on the rate of reduction. Theoretical studies have demonstrated that additional energy resulting from the twins can be remedied by increasing surface coverage of the {111} facet while the seeds are comparatively small. The low surface energy of {111} facet cannot compensate extra strain energy when the seeds are bigger; therefore, producing single-crystal cuboctahedrons as shown in Figure 1[58].

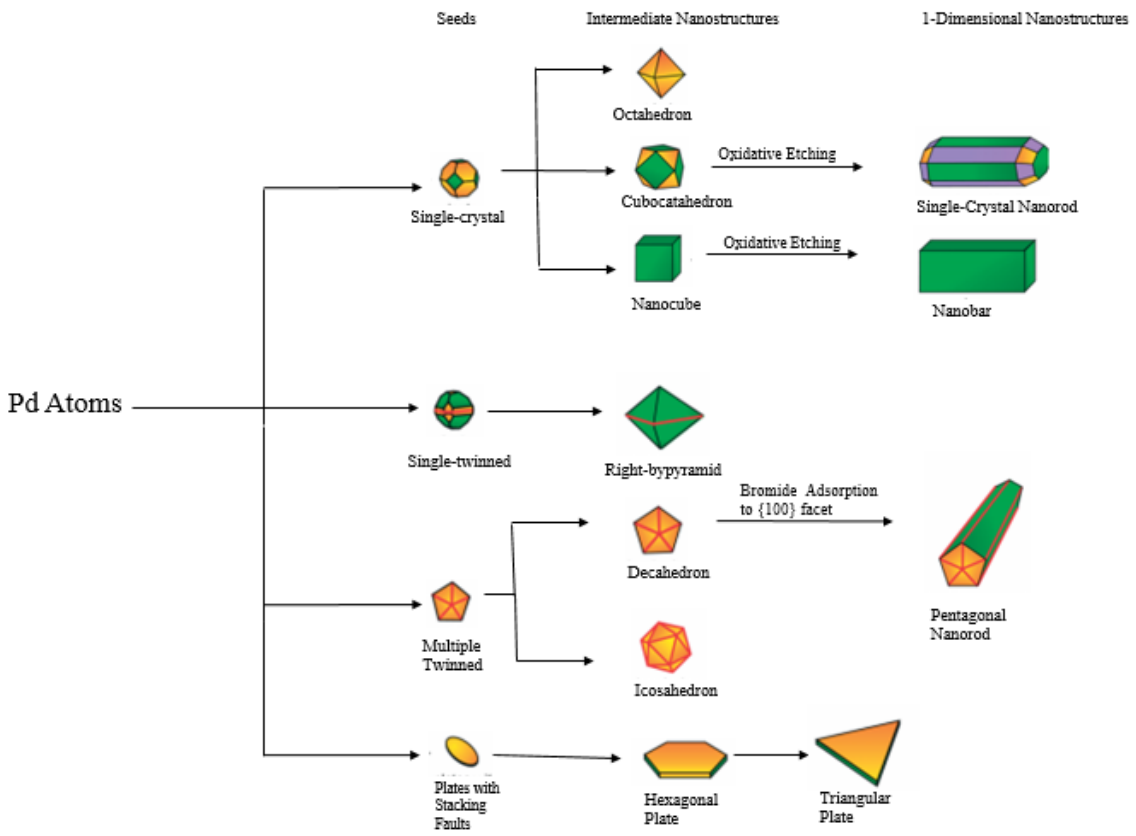

Figure 1: Routes for synthesis of various Pd nanostructures.
Xiong et al.[58]

The type of nanostructures being synthesized is determined by whether the reaction is thermodynamically or kinetically controlled. Under very slow reduction rate, synthesis is kinetically controlled due to the very low concentration of Pd atoms aggregating to the seed structures with minimum surface energy favored by thermodynamics, which consequently results in the in formation of stacking fault in the seeds and formation of nanoplate-like structures. Under thermodynamic control synthesis, the synthesizing nanostructures attempt to minimize the total surface energy by favoring production of structures such as single-crystal and multiple twinned structures at the nucleation and seed formation phases. Reactions under thermodynamic control take place in relatively faster reaction rates. Among decahedrons and icosahedrons as intermediate products of multiple twinned seeds, decahedrons in particular are important for the synthesis of Pd nanorods because the capping of {100} facet of these structures result in internal

strain in the lattice structure that leads to 1D growth in an effort to reduce the total surface energy. These structures ultimately grow into the desired pentagonal Pd nanorods. Based on the route of Pd nanostructure synthesis, the rate of reduction needs to be sufficiently quick to permit thermodynamic control while facilitating slow release of Pd atoms necessary for the nanorod growth[59].

In a thermodynamically controlled synthesis, single crystal and single twinned structures may also be formed but these structures do not contribute to the 1D Pd nanostructure synthesis, which means the multiple twinned structure production must be maximized. The ratio of single-crystal to multiple-twinned seeds can be further manipulated by introducing or preventing oxidative etching. Oxidative etching is primarily caused by both O_2 and chloride ions, which means minimizing the presence of air in the reaction mixture will help maximize the synthesis of multiple twinned seeds and corresponding intermediate structures such as decahedrons[29].

Reaction Parameters Effect On Green Synthesis of Pd Nanorods

Effect of pH Level

The pH level of the solution effects the reduction of Pd precursor. At acidic pH levels (pH 3-4), Pd cannot be completely reduced to metallic Pd based on UV-vis data [60]. Metal ion reduction occurs most efficiently at more neutral pH levels (pH 6-8) as UV-vis spectra from this range resulted in rapid disappearance of absorption peaks denoting Pd precursor. The absorbance at 425 nm corresponds to the $PdCl_4^{2-}$, which is the predominant species of Pd ion that is present in Na_2PdCl_4 solution. Alkaline conditions (pH 10) are also unfavorable towards the formation of Pd

nanoparticles, as Pd-hydro complexes are synthesized instead of metal nanoparticles. Neutral conditions also result in more stable Pd nanoparticles as demonstrated by Pd nanostructures synthesized at pH 6 being stable for over a year[60]. The pH level also affects the particle size of nanoparticles. More alkaline pH conditions resulted in larger Pd nanoparticles[61]. Larger nanostructures may be synthesized at pH levels greater than 5.

Effect of Temperature

Higher temperatures were observed to result in production of more Pd nanoparticles as evidenced by the greater number of Pd nanostructures present in the images obtained from TEM microscopy. This can be attributed to the greater reduction rate resulting from the higher temperatures. No significant change in shapes of the nanoparticles were observed despite change in temperature. The greatest amounts of nanoparticles were synthesized at about 80 °C, after which larger nanostructures could be achieved due to progression of Ostwald ripening[60]. Because of Ostwald ripening, fewer nanostructures are synthesized due to the larger dimensions of the nanostructures. Based on this observation, reactions at high temperatures could result in 1D nanostructure with a high aspect ratio facilitated by Ostwald ripening. The amount of nanoparticles synthesized also increase with more heat[61].

Effect of Reagent Concentration

Reagent concentration can affect sustainable synthesis of Pd nanoparticles in two ways, the increase in concentration of reducing agent, and the increase in precursor concentration. Higher concentration of Pd precursor resulted in smaller average Pd nanoparticles with more uniformity in size distribution[62]. The high concentration of Pd precursor resulted in higher rate of ion reduction. This results in disruption of Ostwald ripening process which is caused by different biological molecules that slow down nucleation through protective effects. Therefore, nanoparticle aggregation was avoided resulting in uniformly separated and well aligned nanoparticles. At lower Pd precursor concentrations, the reduction rate is slower; therefore, the Ostwald ripening occurs more freely. This caused smaller nanoparticles to aggregate with the larger more stable ones in an attempt to reduce the surface energy. Detachment of surface atoms of the smaller particles also occurred. This results in bigger nanoparticles that are closer to the average size for the resulting nanoparticles, thus resulting in more uniform nanoparticles[63 48]. Greater concentrations of green reducing agents, while maintaining constant Pd precursor levels, resulted in greater amounts of Pd nanoparticles until the reducing agent molecules reached equilibrium with metal ions present and until all Pd precursor can be reduced into metallic Pd[64]. The efficiency of precursor reduction can be found by calculating the amount of reducing agent required to completely reduce a specific amount of metal precursor. This would be determined by the Pd precursor concentration present and the chemical formula of the redox (reduction-oxidation) reaction. This can however, be complicated when multiple compounds acting as reducing agents are present. This is common for many natural extracts used as reducing agents.

Effect of Surfactants and Stabilizers

Surfactants and capping agents can be added to improve the Pd nanostructure synthesis process. Capping agents work by changing the order of free energies of different facets of the metal surface via chemical interactions. This can affect the relative growth rates of each facet and could result in distinct shapes as the final product. Bromide ions can be an effective capping agent for Pd, as they chemisorb themselves to the {100} facet of Pd nanocrystals and would result in nanocubes and nanobars[29]. Other capping agents can be employed and distinct synthesis of specific nanostructures based on the facet with which it interacts. For example, the hydroxyl groups of citric acid interacts with {111} Pd facet; thus, resulting in icosahedrons, octahedrons, and decahedrons[29 39]. Surfactants can also be added in the synthesis process to prevent the agglomeration of Pd nanoparticles. Similarly, the requirement to add a separate capping agent may be avoided, as some biological molecules present in green reducing agents could fulfill the same function[65 42].

Suitable Green Reducing Agent for 1D Pd Nanostructure Synthesis

A suitable reducing agent has to be selected based on previous conducted studies that successfully synthesized Pd nanorods. Based on the literature review, riboflavin[7], clove oil[57], and ascorbic acid[30] were reducing agents successfully used in the production of Pd nanorods. Riboflavin, commonly known as vitamin B2 can be extracted from many natural sources such as fruits, and is also available in its pure form as a food supplement and additive. Clove oil is an essential oil extracted from the Syzygium Aromaticum tree leaves and flower buds. Up to 90% of clove oil is

composed of eugenol that acts as a reducing agent. L-ascorbic acid commonly known as vitamin C is also widely available in many natural sources including citrus fruits. It is also available in the form of a supplement and as an additive in its pure form. L -ascorbic acid reduces metal ions by being oxidized into dehydroascorbic acid thereby donating electrons for the reduction reaction.

Segmented Flow Synthesis of Pd Nanorods

Attempts at using continuous flow reactors to synthesize Pd nanostructures have used both synthetic reducing agents such as ethylene glycol, and sustainable reagents such as ascorbic acid. The use of segmented flow consisting of reaction solution droplets immersed in a carrier fluid is also common. Compartmentalized flow promotes better heat transfer and reagent mixing due to the internal convection in the liquid droplets. One such attempt involved using a microfluidic reactor to synthesize very uniform Pd nanocubes using a millifluidic reactor. The reaction mixture was in aqueous medium, but droplets of the mixture were carried by silicone oil[66]. The same concept has been repeated in millifluidic reactors with silicon oil as the carrier fluid to synthesize nanostructures of different metal types including Pd[67]. Cross-flow filtration devices have also been incorporated to these reactors to separate silicone oil from the aqueous suspension of synthesized palladium nanostructures[68]. Using a gas as the carrier fluid would be a very attractive alternative to an immiscible liquid carrier medium like silicone oil, because no oil-aqueous separation process is necessary. Air has been used as the carrier medium and also resulted in the synthesis despite the aspect ratio of the resulting nanorods being low. The experiment used ethylene glycol as reducing agent and solvent[69]. Pd nanorods synthesized this way demonstrated catalytic behavior towards the hydrogenation of styrene to ethylbenzene[23]. None of the studies produced nanorods of high aspect ratio sustainably. Nanorods were either synthesized using a glycol, or other nanostructures such as

nanocubes were produced. The compartmentalized flow in a continuous flow reactor could be obtained more conveniently without the need to add a separate carrier liquid or gas. This involves implementing the experiment at boiling temperature in a millifluidic channel to generate liquid compartments. In this scenario, the solvent will partly vaporize and act as the carrier medium transporting the liquid segments in the reactor. A convenient, sustainable, and efficient approach to Pd nanorod synthesis is to use a millifluidic reactor at boiling temperature with ascorbic acid as the reducing agent in an aqueous solution.

Applications of Pd Nanorods Synthesized Using Green Reducing Agents

Catalysis

Pd is widely used in industry as a catalyst in hydrogenation, hydrogenolysis, and coupling reactions. In order to increase the Pd surface area exposed to the reacting molecules while conserving the amount of valuable metal used, Pd is typically supported on another material, with carbon being the most common. At the nanoscale, the surface area to volume ratio is much higher than with larger structures; therefore, Pd nanoparticles are an alternative to Pd catalyst supported on carbon. The production of carbon supported Pd catalyst is not sustainable as it involves the use of highly toxic formaldehyde as a reducing agent for its synthesis[70] [71]. Pd nanoparticles that demonstrate catalytic behavior and are synthesized using a green reducing agent may be a sustainable replacement for these conventional catalysts. Catalytic Pd nanoparticles synthesized via green reducing agents had a high degree of uniformity , and therefore, were very effective catalysts because the effectiveness factor of catalysts improve as size of particles become more uniform[72] [53]. Another characteristic aspect of catalytic Pd nanoparticles synthesized by green

reducing agents is their high recyclability. The nanoparticles were collected at the end of each reaction cycle, and used again multiple times, which makes them highly desirable as catalysts[73].

Sensors and Energy Storage

Pd nanostructures synthesized using green reducing agents were found to have very high energy density[74]. This would make palladium nanoparticles an ideal material for manufacturing electrodes that store high amounts of energy and show interesting electrochemical properties. Energy storage devices that can possibly be manufactured using such electrodes include symmetric super-capacitors and electrochemical sensors capable of recognizing compounds such as sodium lauryl sulfate (SLS) and Moxifloxacin Hydrochloride (MOXI)[75]. Green synthesized Pd nanowires have also been used to manufacture sensors[76]. Pd nanowires have highly specific surface areas, demonstrate catalytic behavior, and have been used to manufacture an immunosensor capable of detecting carcinoembryonic antigens. The Pd would catalyze a reaction between SLS and MOXI decorated on the surface of the nanowire in the presence of this antigen, resulting in the emission of electrochemiluminescence (ECL) signals[77]. The higher the concentration of the antigen, the greater the intensity of ECL.

Antibacterial and Anticancer Activity

Pd also demonstrates antibacterial and anticancer behavior[78] [49]. This makes palladium a valuable material that can be used in medical applications to mitigate bacterial pathogens and cancer. The higher surface area to volume ratio of nanostructures would be beneficial in these applications because this causes more of the Pd surface area to be exposed to pathogens and cancer cells. Pd could also be easily introduced into the bodies of humans or animals in the form of nanostructures, for example through injection[79]. The use of green reducing agents has been studied as the most prominent sustainable route for the synthesis of Pd nanostructures with anticancer and antibacterial properties. Green reducing agents have been used to synthesize Pd nanostructures that show anticancer activity towards lung[80], kidney[81], ovarian[82], and leukemia[83] cancer cells. Pd nanostructures have also been similarly synthesized to display antibacterial behavior towards the food contaminant *E.Coli*[84] and urinary tract infectant *E.faecalis*[85]. A key advantage of using natural extracts as reducing agents to manufacture Pd nanoparticles for medical applications is that many of these reagents are edible; therefore, the presence of any unreacted reagent in the nanoparticles is safe. Conversely, the use of other reducing agents such as ethylene glycol is unfavorable, as some of them are toxic and harmful to human and animal health, which means the presence of such reagents even in trace quantities in Pd nanoparticles is dangerous.

CHAPTER III
REVIEW OF LITERATURE – PD NANOROD SYNTHESIS USING VIRAL BIOTEMPLATES

Tobacco Mosaic Virus

Tobacco Mosaic Virus (TMV) is a rod-shape virus with a length of 300 nm and a diameter of 18 nm. The protein subunits are helical with 49 subunits in 3 turns of the helix. There are three nucleotides bound to each protein. These coat proteins are primarily alpha-helical with orientation perpendicular to the axis of the particle. In real TMV, the RNA is embedded deep in its structure, roughly at 4 nm of radius from the coat protein. The coat protein consists of about 2,130 replicants of a protein with a molecular weight of 17,500 g/mol that are assembled like bricks in a chimney. Additionally, a secondary protein known as the Hystenine protein with a molecular weight of 26,500 g/mol is also present at a level of about one particle per virion[86].

Barely Stripe Mosaic Virus

Barely Stripe Mosaic Virus (BSMV) consists of a protein helix roughly of 210 to 230 nm in length with 26 coat protein subunits per each turn and a pitch of about 25 nm[87]. The core of the coat protein structure consists of a hollow channel of between 3 and 4 nm in diameter. The RNA is placed at a radius of about 63 angstroms with each coat protein bound to 3 nucleotide residues. The BSMV coat proteins are very similar to those of TMV but they lack axial contacts (these are links between the coat proteins of the virion that are oriented axially) unlike TMV. Instead of

axial contacts BSMV has high radius lateral inter-subunit contacts. Two types of BSMV virions have been identified, which includes the narrow and wide varieties. The main difference between these two types are their diameters that are 21.6 and 22.4 nm, for narrow and wide respectively. The two varieties display 106 and 111 subunits per period in the helix for narrow and wide virions, respectively.

The most significant difference between TMV and BSMV is that BSMV consists of three additional insertions, including one in the inner channel, a second protruding from hydrophobic core and the third at the N terminus, on top of the hydrophobic core. BSMV coat proteins have a literal distance of 7 angstroms each, causing the subunits to be more horizontal relative to TMV[87]. BSMV CP also has a higher degree of lability (likelihood of undergoing chemical change) compared to TMV CP therefore BSMV CP is less stable compared to TMV CP[88].

Benefits of Virus Like Particles

Rod-shape plant Virus Like Particle (VLP) structures with a hollow core open up the structure, making the inner walls of the protein complex available for modification[89]. The hollow space could also facilitate the transport of molecules for applications like drug delivery[90]. This feature encourages further investigation into the structure and behavior of these molecules. Viruses can be expressed in cell cultures while modifying the protein walls of the resulting VLPs, which allows the VLPs to self-replicate. TMV-VLPs can be made capable of self-replication despite the lack of the RNA backbone through mutations in repulsive carboxylate residues E50Q and D77N. This means unlike real viruses that are affected by the recombination and construct instability of the genome that can increase the time required for replication, VLPs expressed in cellular media such as *E. coli*, replicate in the absence of these issues, drastically shortening time for expression and assembly. In TMV-VLPs expression, particles can be produced in 48 hours when compared

to the typical three weeks of real virus production[89]. Facilities such as a greenhouse might be required to cultivate plants for the purpose of obtaining the living plant viruses. This needs additional effort and resources for the management of a greenhouse and cultivation of plants[91]. Obtaining real animal viruses can be even more complicated, as this would require raising animals and infecting them with viruses as a means of replicating them. This would also require additional expertise in animal husbandry and involve many moral and ethical issues[92]. However, these problems are avoidable if virion replication is done using VLP expression in cellular media.

TMV and BSMV as Biotemplates for Pd Nanorod Synthesis

Direct Deposition of Pd on Exterior Surface of TMV

Certain metals such as palladium, silver, gold and platinum could be deposited on TMV more easily relative to other metals such as copper, cobalt, nickel and iron. This is due to the ability of these metal ions to form electrostatic bonds with the TMV coat proteins. Several studies have investigated the deposition of gold particles on the surface of TMV. This includes pH controlled electrostatic binding of gold nanoparticles using several Au precursors including potassium chloroaurate ($KAuCl_4$) with citric acid[93] and $KAuCl_4$ in the presence of acetic acid and Sodium borohydride ($NaBH_4$) as an external reducing agent to reduce the gold ions to gold atoms on the surface of TMV to obtain nanorods[94].

Thick-shelled silica-coated TMV has also been used for synthesis of silver, gold, palladium and platinum nanorods. Thick-shelled silica-coated TMV was initially prepared and incubated in mercaptopropyl trimethylsilane (MPS). The modified virus was centrifuged and resuspended in

(3-(*N*-morpholino) propanesulfonic acid) ($C_7H_{15}NO_4S$) (MOPS) buffer. This mixture was then incubated with metal precursors such as silver perchlorate ($AgClO_4$), hydrogen tetrachloroaurate ($HAuCl_4$), potassium tetrachloroplatinate (K_2PtCl_4), and sodium tetrachloropalladate (Na_2PdCl_4), to synthesize corresponding metal nanorods[95]. Platinum, gold and silver nanorods could also be synthesized without silica modification on TMV[96].

Multiple layers of palladium were also deposited on to the surface of TMV via multiple mineralization cycles without any reducing agents, using sodium tetrachloro-palladate (II) (Na_2PdCl_4) as palladium precursor to deposit palladium on the TMV surface in deionized water for 30 minutes at 50°C[97 98]. A two-step process is necessary for depositing metals that do not attach themselves readily to TMV coat proteins. This procedure requires a metal that attaches more readily to be first deposited on the TMV followed by electroless deposition of the other metals. Typically, the initial layer of metal deposition consists of palladium nanoparticles. The palladium nanoparticles deposited on the coat protein will act as catalytic sites for the formation of the copper, cobalt, nickel and iron coating[99 100].

Synthesis of 3nm Thin Pd Nanorods by Pd Deposition in TMV Viral Channel

Metal nanoparticles can also be deposited in the central channel of TMV. The same techniques of directly decorating the TMV walls with electroless deposition can be used for metals such as palladium, silver, gold, and platinum, while an initial step of palladium mineralization is used for the deposition of nickel, iron, cobalt and copper. However, all comprehensive studies on this method of nanorods production have focused on the second group of metals. TMV was incubated with aqueous Na_2PdCl_4 solution, and an excess of sodium chloride to avoid palladium oxo- and hydroxo- complex formation. The electroless solution also contained DMAB, triethanolamine,

and EDTA. DMAB reduced the Pd^{2+} ions in the viral channel to metallic palladium that could then act as a catalytic site for copper nanoparticle deposition. EDTA acted as the complexing agent and triethanolamine was used as a buffering agent. The buffering agent kept the pH level of the solution constant, therefore compensating for the loss of OH- ions caused by electroless metal deposition. It was found that 40% to 50% of each TMV particle was metallized with copper[101].

Alloyed metal nanorods have also been produced by metal deposition in the viral channel. TMV was dialyzed against Millipore water and then incubated with aqueous Na_2PdCl_4 and an excess of NaCl. After centrifugation, the resulting precipitate was re-suspended in Millipore water. Electroless deposition of metals were prepared by DMAB, sodium succinate, and corresponding metal salts. Cobalt sulfate, iron (II) sulfate and nickel (II) acetate were used in this solution for the deposition of cobalt, iron and nickel, respectively. It was synthesized using CoFe, CoNi, FeNi, and CoFeNi nanorods[102 103].

BSMV as Biotemplates for Pd Nanorod Synthesis

BSMV has been used less when compared to TMV for the production of metal nanorods. However, BSMV is a promising candidate as biotemplate for metal nanorods production. For the first time, Adigun et al. used BSMV as biotemplate for palladium mineralization. The process was carried out in a continuous stirred tank reactor (CSTR). 0.035 mg/ml BSMV and 0.75 mM Na_2PdCl_4 solutions were added to the reactor. The reaction was initiated and 400 microliter aliquots were collected periodically as the reaction proceeded. The samples were then filtered through Acrodisc syringe filters. However, the first palladium particles coating was found not to cover the entire virion even after twenty minutes of incubation. Therefore, the recovered virion-palladium structures were washed and incubated multiple times with tetrachloropalladate.

Resulting nanorods were similar to those with palladium nanoparticles decorating the outer surface of TMV[32].

TMV and BSMV VLPs as Biotemplates for Pd Nanorod Synthesis

Another development in using rod-shape viruses for the production of metal nanorods is the application of corresponding VLPs instead of living viruses. In the case of rod-shape viruses like TMV and BSMV, the VLP counterparts lack the genome; therefore, the central channels of the virions are empty. This can be a helpful feature if the central channel of the virion is used as a template for the production of nanorods. The lack of a genome would free up space for the metal atoms to deposit themselves without disruption. The coat proteins of these VLPs are identical to those of the real viruses, and metal particle deposition on their surfaces also takes place in a similar way. Wnek et al. tried this approach to produce gold nanorods. TMV-VLPs were expressed in *E-Coli*, harvested, and then subjected to ultrasonic lysis. The VLPs were purified by size exclusion chromatography. The TMV-VLPs were dialyzed in buffer solution and then incubated with chloroauric acid and hydroxylamine for the electroless deposition. There was no chemical reducing agent used in the experiments, instead the mixture was exposed to ultraviolet radiation for photoreduction. This would cause the gold ions deposited on the exterior surface of the TMV-VLPs to be reduced to metallic gold thus producing gold nanorods[104].

Applications of Pd Nanorods Synthesized Using Viral Biotemplates

Catalysis

When more surface area of a catalyst is exposed to reactants, they are more efficient because more active sites are present for reacting molecules. A cheaper alternative to using large quantities of precious catalytic metal is for the catalyst to be deposited on an inexpensive inert substrate with a high surface area to volume ratio such as a biotemplate. Pd catalyst synthesized by assembling TMV1cys on a gold substrate with nanostar configuration resulted in an increase in reaction rate of 68% compared to commercial Pd/C catalyst of similar size.[61] Catalysts synthesized by TMV biotemplates can be recycled over multiple cycles without a significant drop in efficiency[4, 5, 61]. The superior performance of catalyst mineralized on TMV is primarily due to two reasons. Palladium atoms mineralized on TMV are more uniform compared to conventional palladium catalysts supported on carbon substrates, therefore demonstrate better catalysis[61, 62]. The deposition of palladium on TMV surface also does not require external surfactants or capping agents, therefore active sites are not blocked unlike with conventionally synthesized Pd catalysts[63]. Removing these surfactants also contributes to increased cost of manufacturing the catalyst and the process could be incomplete. Biotemplated Pd catalyst shows better catalytic activity and is cost effective.

Sensors

Efficient sensors need to be highly selective, sensitive, and structurally stable over a wide array of background conditions. Selectivity for a molecule in mixed samples is obtained through viral

surfaces functionalized with metals, enzymes or other chemicals. For example, TMV coated with Pd can rapidly and reversibly detect hydrogen molecules at room temperature[50]. Gold-coated nanorods also conjugate with folic acid by coupling agents that interact with the folate receptors on tumor cells. This could be used to effectively detect cancers [19]. TMV was coated with biotin to allow binding of enzymes that facilitate detection of penicillin [64]. Desirable properties like sensitivity and stability are resultant from the nature of viral biotemplates. High surface area to volume ratio of TMV result in more contact with the molecules being detected, therefore amplifying signal generation to improve device sensitivity[65]. The TMV structure is also very stable at high temperatures and over a bigger range of pH levels that they encounter during detection. Therefore, biosensors synthesized from TMV biotemplates are more durable and effective.

Batteries

TMV virions with metal coating can be vertically assembled on a gold substrate to form a nanoforest structure to generate currents. The vertical assembly of virions is possible due to introduction of a cysteine residue at amino terminus of coat protein to synthesize TMV1cys [3 6]. Most cysteines in TMV are not able to bind into metal; however, the N-terminal residue is open to vertical assembly of the virion on the gold substrate by covalent interactions between gold and the cysteine's thiol group. Additionally, nickel or cobalt coating increases the active electrode surface area by about tenfold and electrode discharge capacity is doubled [3]. TMV anodes with Pd, Ni or Si coatings in lithium ion batteries causes discharge capacity to rise by tenfold compared to graphite anodes[6]. TMV incorporated sodium-ion batteries use TMV coated with carbon, tin or nickels as anodes to increase battery cycling lifespan with minimal reduction at charge capacities

over 150 charging cycles[30.] TMV coated pattern with similar nanoforest structures have also shown to increase efficiency of micro-supercapacitors that use electrode surface area to store charge.[60]

CHAPTER IV
EXPERIMENTAL APPROACH – PD NANOROD SYNTHESIS USING GREEN REDUCING AGENTS

Material

Materials and reagents that were used in the experiments include L-ascorbic acid (Sigma Aldrich 1002892452), Na_2PdCl_4 (Sigma Aldrich 1003067874), KBr (Sigma Aldrich 102252504), poly(vinyl pyrrolidone) (PVP) (Sigma Aldrich 102034133), Eugenol (Aldrich E51791-100G), Riboflavin (Sigma R9504-25G), Deionized Water (LabChem LC267505) and silicone oil (Fisher Chemical S159-500).

Selecting A Suitable Green Reducing Agents

Synthesis

Riboflavin, Clove oil, and L-ascorbic acid were tested to identify the reducing agent most promising for synthesizing Pd Nanorods. A batch reaction for each reducing agent was conducted and TEM images of the synthesized Pd nanostructures were used to choose the most suitable reducing agent for synthesizing Pd nanorods. 50 mg of riboflavin was dissolved in 20 ml of aqueous solvent and heated in a three-neck flask in a water bath at 50°C with stirring. 2 ml of

aqueous 10 mM Na_2PdCl_4 was added to the riboflavin solution and allowed to react for 1 hour. Eugenol had to be diluted in ethanol at a ratio of 1:200 due to its insolubility in water. 30 ml of this solution was added to a three-neck flask in a water bath and allowed to heat at 70°C with stirring. 5 ml of 0.2 mM aqueous Na_2PdCl_4 was added to the eugenol solution, and allowed to react for 30 minutes. Batch synthesis of Pd nanostructures using ascorbic acid is explained in the following section of this thesis, since ascorbic acid was the only reducing agent that successfully synthesized Pd nanorods among the three initially tested green reducing agents[105].

Batch Synthesis of Pd Nanostructures Using L-Ascorbic Acid

In Pd nanostructure synthesis using L-ascorbic acid as the reducing agent, Na_2PdCl_4 is used as Pd precursor, KBr as capping agent, and poly(vinyl pyrrolidone) (PVP) as the stabilizer. Two aqueous solutions were made. The first consisted of 31 mM of L-ascorbic acid and 87 mM of PVP. The other solution consisted of 17.4 mM Na_2PdCl_4 and 460 mM of KBr. A 35 ml three-neck flask was used in a silicon oil bath seated on a hot plate with stirring at 150 rpm. The Na_2PdCl_4 and KBr solution was added first to the reaction vessel, followed immediately by the

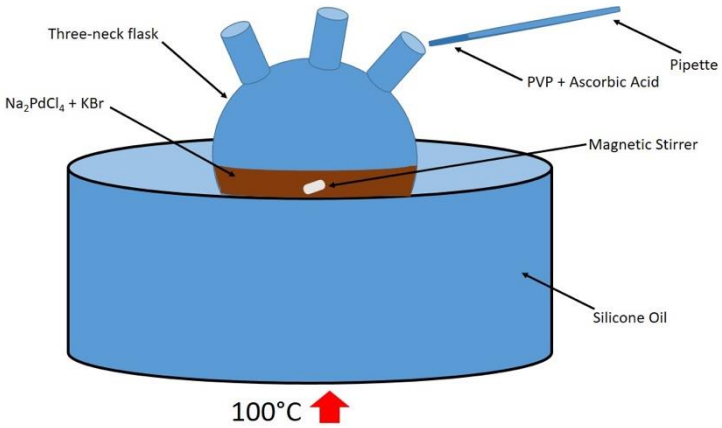

Figure 2: Batch reactor set-up for Pd nanostructure synthesis using L-ascorbic acid.

solution of PVP and L-ascorbic acid. 5 ml of each solution was used and the reaction was run at 100°C for 3 hours. Once the batch reactions were complete, the sample was cooled in an ice bath for a few minutes. A schematic of batch synthesis of Pd nanostructure using L-ascorbic acid is illustrated in Figure 2.

Continuous - Flow Synthesis of Pd Nanostructures Using L-Ascorbic Acid

Two aqueous solutions were made similar to batch synthesis. In continuous millifluidic synthesis, 5 ml of each solution was pumped through a millifluidic reactor at a flow rate of 0.0067 ml/min using a syringe pump (Chemyx Fusion 200) to achieve a 3-hour residence time. The millifluidic reactor consisted of 4 ft long 1/16'' ID polytetrafluoroethylene (PTFE) tubing which was placed in a silicone oil bath while its temperature was maintained at 100 °C. The boiling reaction solution flowed through the millifluidic tubing as segmented flow. Liquid segments consisting of reaction solution, were immersed in the steam generated by the boiling of the solvent water (which acts as the carrier fluid). The synthesized palladium nanostructures were collected into a falcon tube in an ice bath. A schematic of batch synthesis of Pd nanostructure using L-ascorbic acid is illustrated in Figure 3.

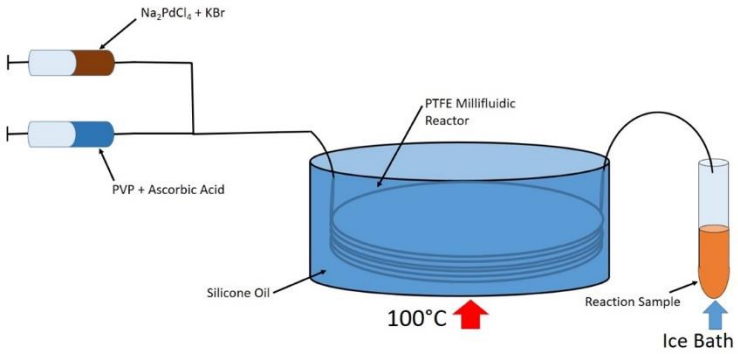

Figure 3: Continuous millifluidic reactor set-up for Pd nanostructure synthesis using L-ascorbic acid.

Parametric Study of Segmented Flow of Pd Nanostructures Using L-Ascorbic Acid

Reagent concentrations including Na_2PdCl_4, L-ascorbic acid, KBr, and PVP have a strong effect on size and morphology of the synthesized nanostructures as well as on the yield of 1D nanostructures (nanorods). Their effect on the yield and dimensions of synthesized nanorods can be studied by changing one reagent concentration while other parameters are kept the same. The millifluidic reaction was repeated while halving and doubling each reagent concentration each time to observe effects on the synthesized nanostructures. TEM imaging was used to find the percentage of Pd nanorods synthesized in each experiment and their average lengths. Based on these observations, new reaction parameters were determined to obtain high yields of nanorods. These parameters were used to study the reaction kinetics leading to nanorod synthesis in a continuous flow reactor.

Kinetic Study of Segmented Flow of Pd Nanostructures Using L-Ascorbic Acid

The kinetics study was done using millifluidic reactors with lengths of 1 feet, 2 feet, 3 feet, and 4 feet to repeat the experiment at constant flow rate at 0.0067 ml/min. The resulting sample was collected into a falcon tube in an ice bath and centrifuged at 3000 rpm for 30 minutes. Afterwards, the supernatant was collected and characterized using ultraviolet-visible (UV-Vis) spectroscopy to determine the remaining concentration of $PdCl_4^{2-}$ ions present in reaction solution. The residue from the sample was further washed by multiple cycles of centrifugation and used for TEM imaging. The TEM images of produced nanostructures and UV-Vis characterization of the supernatant were analyzed to calculate reduction rate and understand the reaction mechanism. The reagent concentrations used in this experiment were 17.4 mM Na_2PdCl_4, 87 mM PVP, 12 mM L-ascorbic acid, and 750 mM KBr. These parameters were chosen to maximize the synthesis of nanorods based on observations from the experiments that

studied the effects of different reagent's concentrations. All other reaction conditions including temperature and type of tubing remained the same as the original reaction. A calibration curve was used to convert the UV-Vis absorbance into of $PdCl_4^{2-}$ concentration values. The calibration curve was prepared using the data collected from performing UV-Vis spectroscopy on Na_2PdCl_4 solutions with concentrations of 20mM, 10mM, 5mM and 2.5mM.

Characterization Techniques

TEM Characterization

TEM imaging was performed using a Jeol JEM 2100 microscope on carbon coated copper grids at 200 kV. Samples were washed by 3 cycles of centrifugation, and a tiny drop of the sample was placed on the grid and allowed to dry. The grid was then loaded on to the instrument. The number of nanorods on the TEM images were counted and lengths measured using image-J software.

UV-Vis Characterization

UV-Vis characterization was conducted on samples using a Mettler Toledo UV 5 UV-Vis spectrophotometer. The samples for UV-Vis characterization were prepared by diluting 100 microliters in 1.5 ml of deionized water which was then transferred to a plastic cuvette that was then capped. The Cuvette was placed in the instrument and the UV-Vis spectrum generated. The absorbance at 425 nm wavelength corresponds to the concentration of $PdCl_4^{2-}$ ions in the sample solution which were then measured for further kinetic studies.

CHAPTER V
EXPERIMENTAL APPROACH – PD NANOROD SYNTHESIS USING VIRAL BIOTEMPLATES

Material

Materials and reagents used in the experiments include Na_2PdCl_4 (Sigma Aldrich 1003067874), Lennox Broth (LB) Agar (Fisher Bioreagents BP1427-500), ampicillin (Fisher Bioreagents A5354), chloramphenicol (Fisher Bioreagents R4408**)**, IPTG (Gold Biotechnology I2481C), Lysonase (Millipore 71230), Deionized Water (LabChem LC267505), and Bug-buster (Millipore 70584).

TMV VLP Expression and Viral Purification

BL21 competent *E.coli* cells transformed with TMV plasmid DNA with carboxylate residue modifications E50Q and D77N were readily available, but these cells demonstrated lack of resistance to the antibiotic chloramphenicol. This required plasmid DNA to be extracted from the available cells and used to transform BL21 codon plus competent *E.coli* cells that were resistant to chloramphenicol. The cells were plated on LB agar plates containing chloramphenicol and ampicillin, and incubated at 37 °C. Bacterial colonies were observed on the plate the next day, and a single colony was picked up by a pipette tip to inoculate 3 ml of Lennox Broth (LB) agar

solution containing ampicillin and chloramphenicol which was left in a shaker overnight at 37 °C. An aliquot from this solution was added to larger volume of media to expand the bacterial solution. This solution was also placed in the shaker overnight followed by its centrifugation at 6,500 rpm for 5 minutes to obtain the residue of bacterial cells containing the virions. VLPs were obtained by performing viral purification on these cells. Bug buster, lysonase, and DTT (Dithiotreitol) were the reagents added to the residue procured from the centrifugation to facilitate viral purification, which was then ultracentrifugated at 44,000 rpm for 1 hour. The residue from the ultracentrifugated sample contain the VLPs, and was dissolved in 1M pH 7 phosphate buffer to obtain a solution of stable TMV VLPs that was stored at 4 °C. An estimate of the TMV VLP concentration may be obtained using equation 1 below. The UV-Vis absorbance at the wavelengths of 280 nm and 260 nm were measured that correlate with the concentrations of proteins and nucleic acids, respectively. This calculation adjusts for possible nucleic acid contamination.

$$\text{Concentration (mg/ml)} = (1.55 * A_{280}) - (0.76 * A_{260}) \qquad \text{Equation 1}$$

Batch Synthesis of Pd Nanostructures Using TMV VLP Biotemplates

Two sets of baseline batch reaction conditions were used in the experiments involving both high and low concentrations of reagents while maintaining the ratio of Pd precursor to TMV VLP concentration of 6.7. At 0.5 mM of Na_2PdCl_4, 0.298 mg/ml of TMV VLP solution was used, while at 2 mM of Na_2PdCl_4, 0.304 mg/ml of TMV VLP concentration was employed. The Pd precursor solution was aqueous while the TMV VLPs were in a pH 7 phosphate buffer. The experiments were performed in a three-neck flask while stirring in a water bath on a hotplate. The TMV VLP solution was added to the reaction vessel and allowed to be heated at the reaction temperature for about a minute followed by addition of Pd precursor solution. After 1 hour of reaction at 50°C in the dark, the reaction solution was cooled in an ice bath, and washed with deionized water in three cycles of centrifugation in preparation for TEM imaging. A schematic of batch reaction set-up for Pd mineralization on TMV VLP surface is shown in Figure 4. The batch reaction was repeated with the In-Situ FTIR sensor probe to investigate the activity of the functional groups on TMV VLP capsid protein.

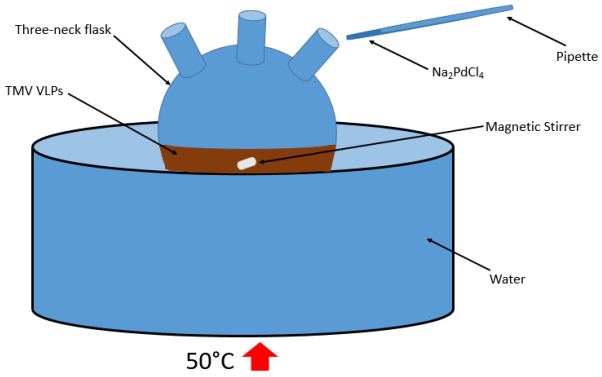

Figure 4: Batch reactor set-up for Pd mineralization on TMV VLP biotemplate.

Characterization Techniques

TEM imaging was performed using a Jeol JEM 2100 microscope on carbon coated copper grids at 200 kV. The samples were negative stained with uranyl acetate after being placed on the TEM grid. Samples were washed by 3 cycles of centrifugation and a tiny drop of the sample was placed on the grid, and allowed to dry. The grid was then loaded on to the instrument. The length of VLPs on the TEM images were measured using image-J software.

CHAPTER VI
RESULTS AND DISCUSSION – PD NANOROD SYNTHESIS USING GREEN REDUCING AGENTS

Selecting Reducing Agents

Pd Nanostructure Synthesis Using Riboflavin as Reducing agent

The experiments conducted in acetone and deionized water resulted in the synthesis of nanorods in the previous study. The experiment using aqueous solvent was chosen to be repeated, as acetone is not a sustainably sourced solvent[7]. The resulting SEM image from the experiment that used the aqueous solution is shown in Figure 5. No Pd nanorods were observed but heavily aggregated Pd nanoparticles were observed; therefore, the experiment was unsuccessful at synthesizing Pd nanorods.

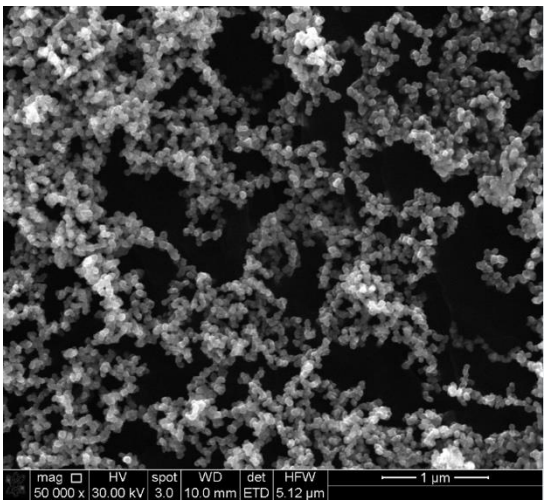

Figure 5: SEM image of Pd nanoparticles synthesized using riboflavin as a reducing agent.

Pd Nanostructure Synthesis Using Clove Oil as Reducing agent

Eugenol as the main constituent compound of clove oil reduces Pd ions by donating electrons from the electron rich phenol ring of the molecule, resulting in the mineralization of Pd. During the reduction reaction, the eugenol molecule is oxidized causing the phenol ring to be a hexagonal ring with two double bonds and the hydroxyl group to become a carbonyl group. The experiment from Matheus et al. was repeated to attempt the synthesis of Pd nanostructures[57]. The SEM images of the resulting sample also showed the aggregation of Pd nanoparticles, and that no Pd nanorods were synthesized by the reaction.

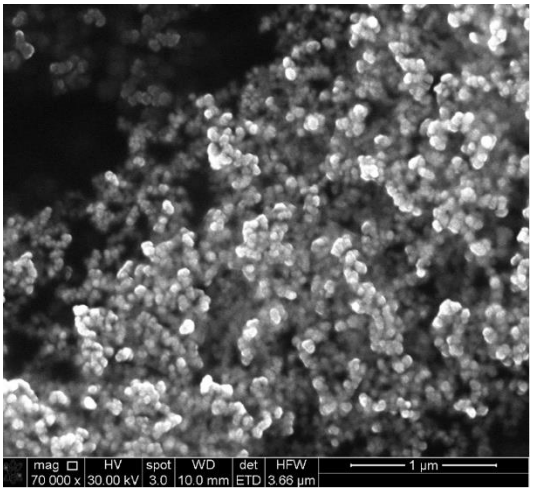

Figure 6: SEM image of Pd nanoparticles synthesized using eugenol as a reducing agent.

Pd Nanostructure Synthesis in Batch and Millifluidic Reactors Using L-ascorbic Acid

L -ascorbic acid reduces metal ions by being oxidized into dehydroascorbic, and donating electrons for the reduction reaction. This was the only reducing agent that successfully synthesized Pd nanorods among the three initially tested green reducing agents[105]. Based on Figure 7, both batch (Figure 7 (a)) and millifluidic (Figure 7 (a)) reactions resulted in the synthesis of nanocubes and pentagonal nanorods. The frequency of nanorod synthesis in the millifluidic reaction (Figure 7(b)) was greater, at over 12% of all synthesized structures, while the

value was only 5% for the batch reaction. There was also more uniform distribution of nanorods in the millifluidic reaction compared to the batch sample, which had the 1D nanostructures clustered only around a few spots on the TEM grid. Higher aspect ratios were also observed in the pentagonal nanostructures synthesized by the millifluidic reactor. The lengths of the nanorods from the millifluidic and batch reactor averaged at about 100 nm and 60 nm, respectively. The greater occurrence of Pd nanorods in the millifluidic reactor could be due to the presence of air in the reaction mixture being minimized in the narrow millifluidic channel. The lack of air prevents oxidative etching, thereby resulting in the synthesis of more multiple-twinned structures such as decahedrons, the seed structures that eventually grow into Pd nanorods.

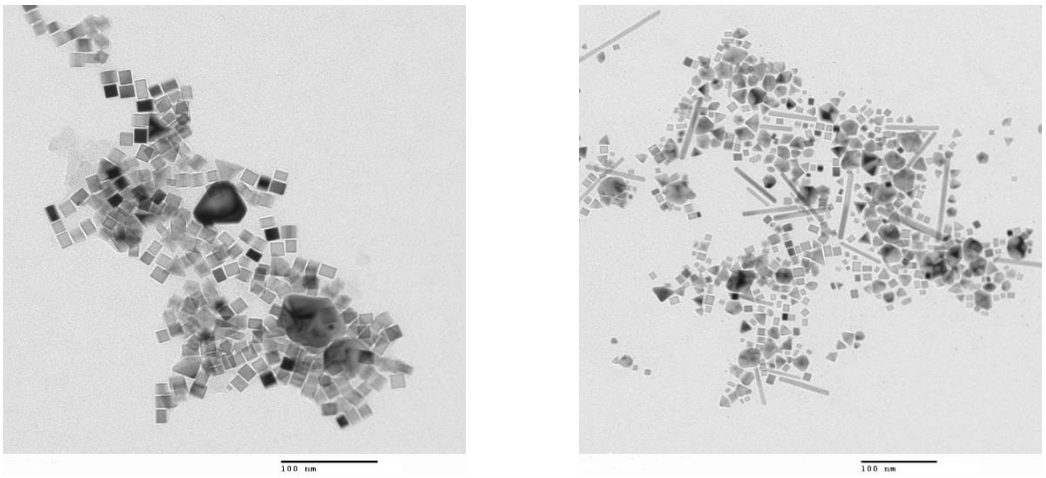

(a) 31 mM of L-ascorbic acid, 87 mM of PVP, 17.4 mM of Na_2PdCl_4, and 460 mM of KBr.

(b) 31 mM of L-ascorbic acid, 87 mM of PVP, 17.4 mM of Na_2PdCl_4, and 460 mM of KBr.

Figure 7: TEM images of synthesized Pd nanostructure in batch (a) and millifluidic (b) reactor.

Parametric Study and Analysis

Effect of Reducing Agent Concentration

The change in the concentration of L-ascorbic acid as the reducing agent also has the potential to affect the size and morphology of the synthesized Pd nanostructures, as well as the yield of synthesized Pd nanorods. The reduction rate needs to be precisely controlled in order to ensure the reduction rate is fast enough for the production of twinned structures such as decahedrons in the nucleation process[106]. The reduction rate also needs to be sufficiently slow to permit the growth of these decahedron seeds into nanorods[105]. Based on Figure 8, doubling ascorbic acid concentration resulted in very few nanorods being synthesized. This could be due to the high reducing agent concentrations that lead to a faster reduction rate. This caused more of the Pd precursor to be reduced during the early phase of the reaction; therefore, less precursor is available during the nanorod growth. This would result in fewer nanorods being synthesized. A decreased reducing agent concentration would lower the reducing rate to a value more suitable for nanorod synthesis. Experiment with lowered ascorbic acid concentrations resulted in a greater percentage of nanorods, confirming this hypothesis as seen in figure 8. Empirically, seed crystalinity is a result of the reduction rate that influences the size of synthesized seeds. Fast reduction of Pd precursor to generate Pd atoms could lead to more single crystals due to their rapid size growth. When reduction is substantially slowed, the multiple-twinned seed sizes can be minimized for a longer time due to the slow atom addition. Multiple-twinned seeds are synthesized in high yields at slow reaction rates, but the reaction rate needs to be sufficiently fast to ensure thermodynamic control of the reaction. Ascorbic acid is an effective reducing agent for Pd nanorod synthesis due to its ability to maintain a balanced rate of reduction that maintains thermodynamic control while permitting Multiple-twinned seed synthesis.

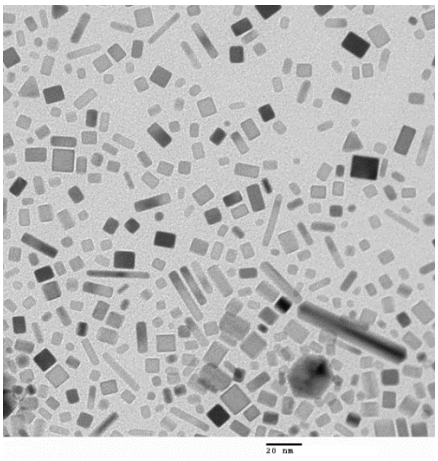

(a) 15.5 mM of L-ascorbic acid, 87 mM of PVP, 17.4 mM of Na_2PdCl_4, and 460 mM of KBr.

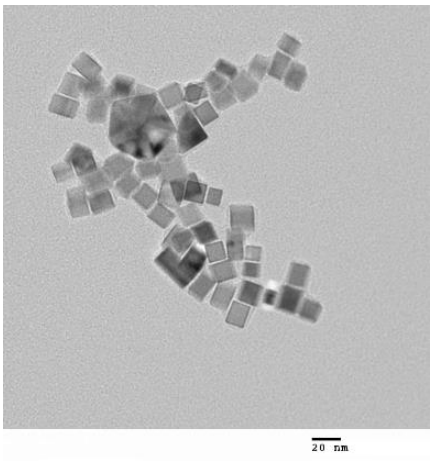

(b) 62 mM of L-ascorbic acid, 87 mM of PVP, 17.4 mM of Na_2PdCl_4, and 460 mM of KBr.

Figure 8: Effect of L-ascorbic acid concentration (a) lower and (b) higher concentration of L-ascorbic on the yield of 1D Pd nanostructures.

Effect of Capping Agent Concentration

The concentration of KBr was doubled (920 mM) and halved (230 mM) from the baseline reaction conditions. The lower concentration of KBr resulted in a lower occurrence of 1D nanostructures, as observed in Figure 9 (a). This demonstrates the capping action of Br^- ions that chemisorb into the {100} facets of decahedrons' seeds as they grow into nanorods[107]. A greater concentration of KBr would cause more Br^- ions being available in the reaction solution causing the chemisorption to occur at a greater frequency. This would result in more decahedrons having their {100} facets passivated; thus, developing into pentagonal nanorods. More KBr also cause decahedrons to develop into longer nanorods. This could be due to the ligand exchange that occurs in the Na_2PdCl_4 and KBr solution, which results in the formation of $PdBr_4^{2-}$ ions that are more stable (about 10^4 times higher stability constant) than the $PdCl_4^{2-}$ [108]. This causes the reduction rate to decrease substantially; therefore, providing more time for the growth of

nanorods resulting in longer structures[59] [52]. When concentration was doubled to 920 mM, a further increase in the amount of the nanorods synthesized was not observed. Instead, a much lower percentage of nanorods were synthesized as seen in Figure 9 (b), and large uneven twinned structures are predominant. This could be due to an excess of Br^- ions combined with high reaction temperature leading to oxidative etching of the seed decahedrons that prevent them from developing into nanorods, and alternatively grow into large uneven twinned structures[109].

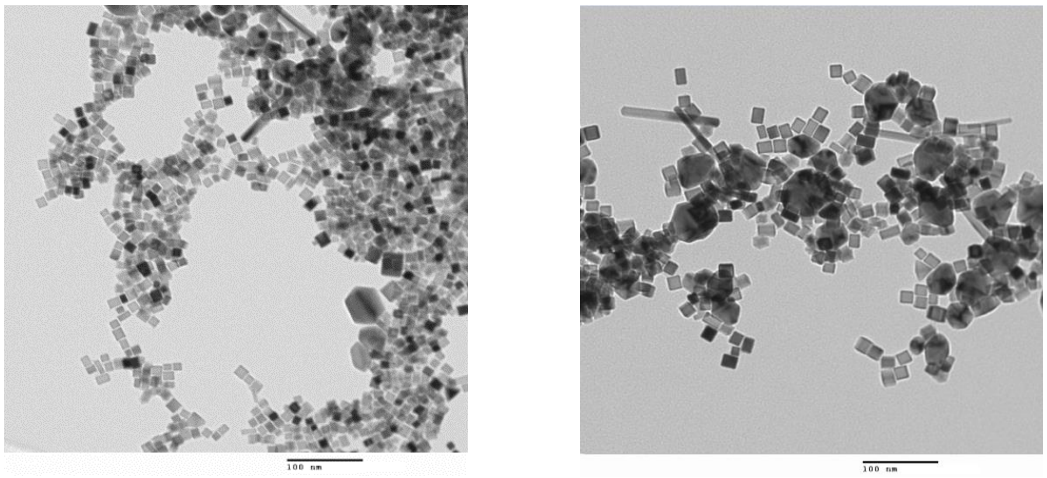

(a) 31 mM of L-ascorbic acid, 87 mM of PVP, 17.4 mM of Na_2PdCl_4, and 230 mM of KBr.

(b) 31 mM of L-ascorbic acid, 87 mM of PVP, 17.4 mM of Na_2PdCl_4, and 920 mM of KBr.

Figure 9: Effect of KBr concentration (a) lower and (b) higher concentration of KBr on the yield of 1D Pd nanostructures.

Effect of Stabilizing Agent Concentration

The effect of PVP concentration was also studied by repeating the millifluidic reaction with doubled (174 mM) and halved (43.5 mM) concentrations from the baseline reaction parameters. Based on Figure 10 (a), decrease in PVP concentration resulted in lower occurrence of Pd nanorods and presence of structures that are visible to be enlarged uneven decahedrons. Based on this

observation, it may be hypothesized that PVP is required to stabilize the surface of decahedrons. Without the stabilizing effect of PVP, the decahedrons enlarge rapidly and unevenly[110]. These larger structures cannot be grown into nanorods through the capping action of Br^- ions; therefore, only a few nanorods are successfully synthesized in the reaction. On the other hand, higher PVP concentration did not significantly change the results from the original reaction. Therefore excess PVP beyond the amount required to control the size of the decahedrons did not affect the experiment's outcome. This observation from Figure 10 (b) corroborates that unreacted surplus PVP in the reaction solution does not interact with the developing nanostructures once their surfaces stabilize.

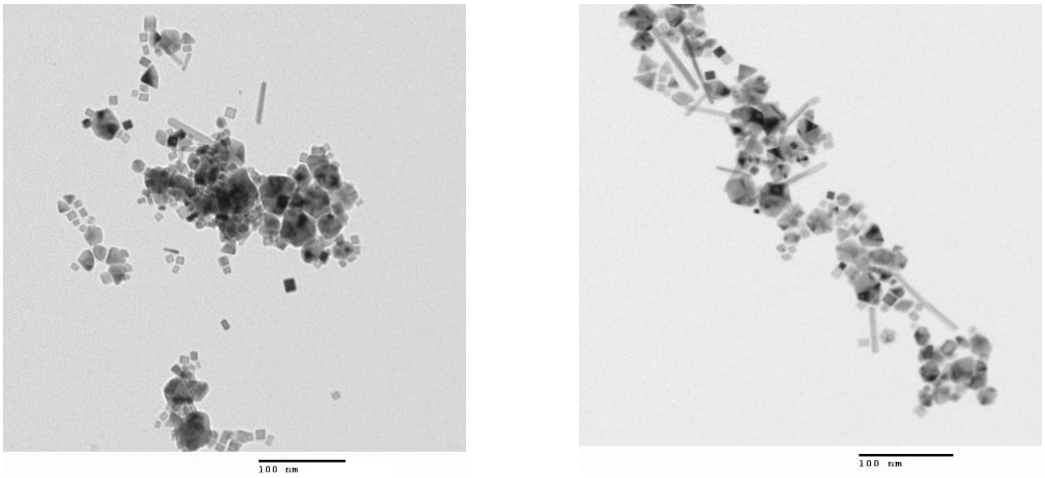

(a) 31 mM of L-ascorbic acid, 43.5 mM of PVP, 17.4 mM of Na_2PdCl_4, and 230 mM KBr.

(b) 31 mM of L-ascorbic acid, 174 mM of PVP, 17.4 mM of Na_2PdCl_4, and 230 mM KBr.

Figure 10: Effect of PVP concentration (a) lower and (b) higher concentration of PVP on the yield of 1D Pd nanostructures.

Kinetic Study and Analysis

This is an investigation on the kinetic parameters that include rate constant and activation energy that is derived from spectroscopy measurements, which can then be used to calculate initial rate

of reduction. Quantitatively, the initial rates of reduction required for Pd nanorod synthesis would be determined. Potentially, the initial reduction rate can be adjusted using reaction parameters such as temperature, and the reduction rate can be correlated with the concentration of multiple twinned seed and percentage of synthesized Pd nanorods. The concentrations of $PdCl_4^{2-}$ ions left in the reaction solution at different points of the length on the reactor that correlate with different points of times of the reaction was used to calculate the rate of reduction.

A calibration curve was created by measuring UV-Vis absorbance at 425 nm for various concentrations of Na_2PdCl_4 as shown in Figure 11. $PdCl_4^{2-}$ ions have a characteristic absorbance peak at 425 nm[111]. The calibration curve can be used to generate a linear coloration that would be used to calculate the $PdCl_4^{2-}$ ion concentration from the UV-Vis characterization of solutions, including those resulting from Pd nanorod synthesis reactions. This is useful in the kinetic study when determining the change in $PdCl_4^{2-}$ ion concentration as the reaction proceeded. This would be necessary to establish a relationship between precursor concentration and time; therefore, determining the route of Pd nanorod synthesis, as well as the reduction rate by which the Pd precursor is reduced by L-ascorbic acid. Studies have been performed in the past with batch experiments[112]. This typically involved collecting samples of the reaction solution at different times as the reaction progressed, followed by a characterization technique such as UV-Vis spectroscopy to determine the metal ion concentration.

This study attempted a new approach to kinetic study by applying the concept into the continuous-flow reactors. Instead of collecting samples periodically from a batch reaction, the experiment would be repeated in reactors of varying lengths. The reaction was performed in reactors with lengths of 1, 2, 3, and 4 feet. The UV-vis spectra for the resulting reaction solutions after separation of nanostructures that were synthesized from each reactor length is displayed in Figure 12. Characteristic absorbance peaks are seen at 425 nm to signify $PdCl_4^{2-}$ ions. Characteristic absorbance at 332 nm confirms the presence of $PdBr_4^{2-}$; therefore, providing

evidence for the ligand exchange reaction taking place in the reaction solution[113]. Ligand exchange is demonstrated by Equation 4. Ascorbic acid as the reducing agent is assumed to be in great excess compared to metal precursor Na_2PdCl_4, and it can be assumed that the concentration of the reducing agent will remain almost constant during the reaction. This makes it possible to approximate the kinetics of the reaction as a pseudo-first-order reaction, and the rate law will be simplified to Equation 2, that can then be integrated into Equation 3. In equation 3, $[PdCl_4^{2-}]_t$ is the precursor ion concentration at the time of measurement, and $[PdCl_4^{2-}]_0$ is precursor ion concentration at the beginning of the reaction. The time passed since the start of the reaction until time of the measurement is represented by t. The reaction constant that is to be determined is k.

$$R = k[PdCl_4^{2-}] \quad \text{Equation 2}$$

$$\ln [PdCl_4^{2-}]_t = -kt + \ln [PdCl_4^{2-}]_0 \quad \text{Equation 3}$$

$$PdCl_4^{2-}(aq) + 4Br^-(aq) \rightarrow PdBr_4^{2-}(aq) + 4Cl^-(aq) \quad \text{Equation 4}$$

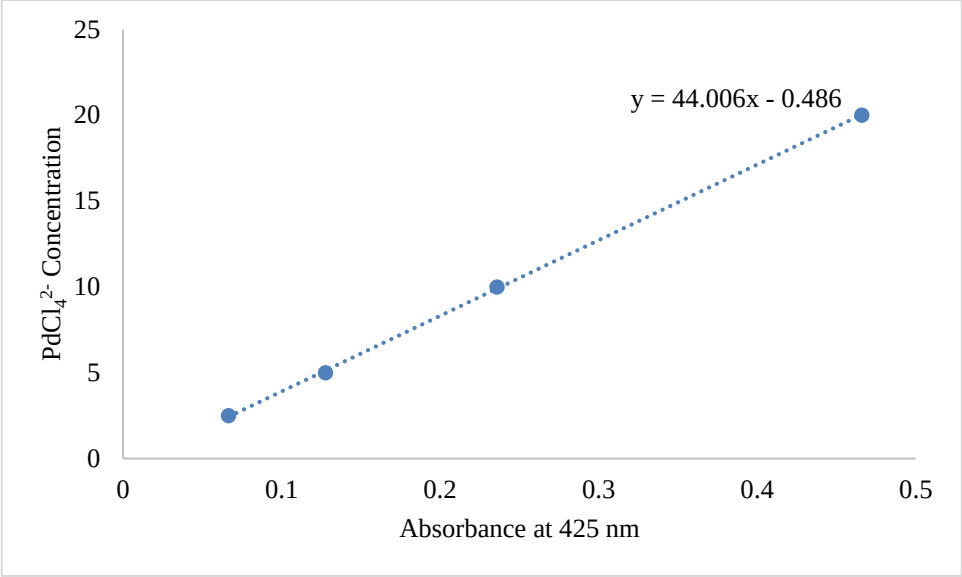

Figure 11: Calibration curve obtained by measuring absorbance at 425 nm wavelength of 20 mM, 10 mM, 5 mM, and 2.5 mM concentration of aqueous Na_2PdCl_4 solutions.

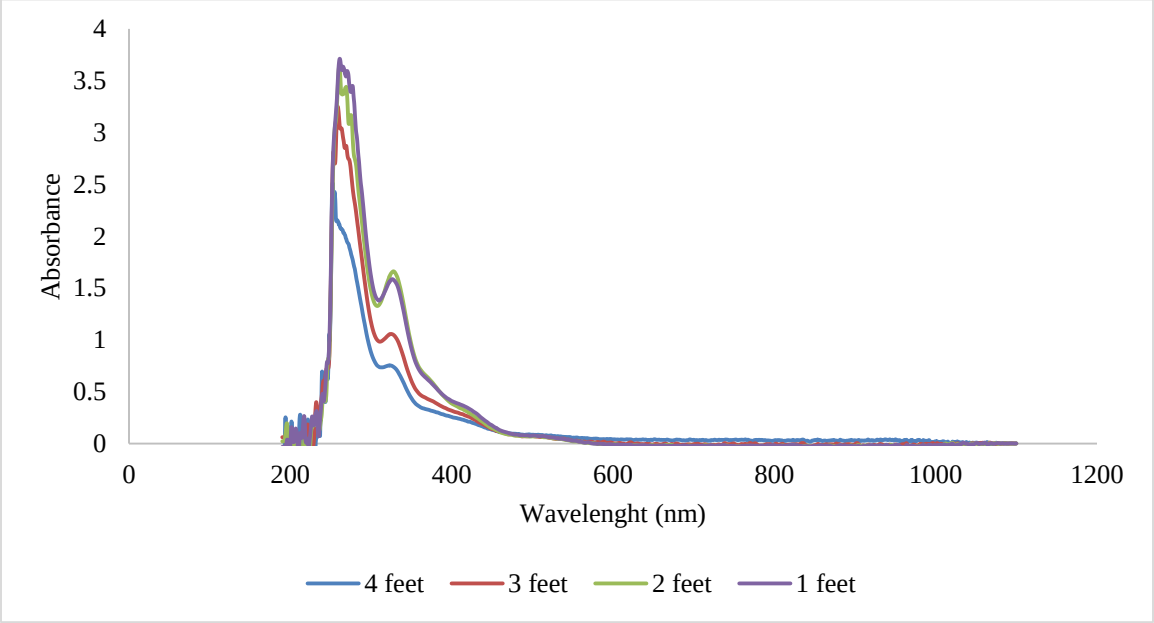

Figure 12: UV-Vis spectra of samples obtained from 1 foot, 2 feet, 3 feet, and 4 feet of millifluidic reactor lengths.

Based on Equation 1, natural log of $PdCl_4^{2-}$ ion concentration versus time graph needs to be constructed for the purpose of finding rate constant. The flow rate is constant for all different reactor lengths; therefore, length of reactor is directly proportional to time passed (residence time). For instance, the 2 feet reactor being half of the length of the full reactor; thus, corresponds to half the residence time. The residence time used in the reaction is 3 hours; therefore, the 2 feet reactor corresponds to 1.5 hours. The sample from each millifluidic reactor experiment was collected and after a single cycle of centrifugation, the supernatant was characterized using UV-Vis. The absorbance at 425 nm was converted to a $PdCl_4^{2-}$ ion concentration using the equation from the calibration curve (Figure 11). These results are summarized in Table 1.

Table 1: Absorbance at 425 nm, and corresponding $PdCl_4^{2-}$ concentration at different lengths of milllifluidic reactor.

Time (sec)	Length (feet)	Absorbance at 425 nm wavelength	$[PdCl_4^{2-}]$ (mM)	ln ($[PdCl_4^{2-}]$)
0	0	0.41	17.40	2.86
2700	1	0.32	13.55	2.61
5400	2	0.28	11.76	2.46
8100	3	0.24	10.22	2.32
10800	4	0.20	8.37	2.12

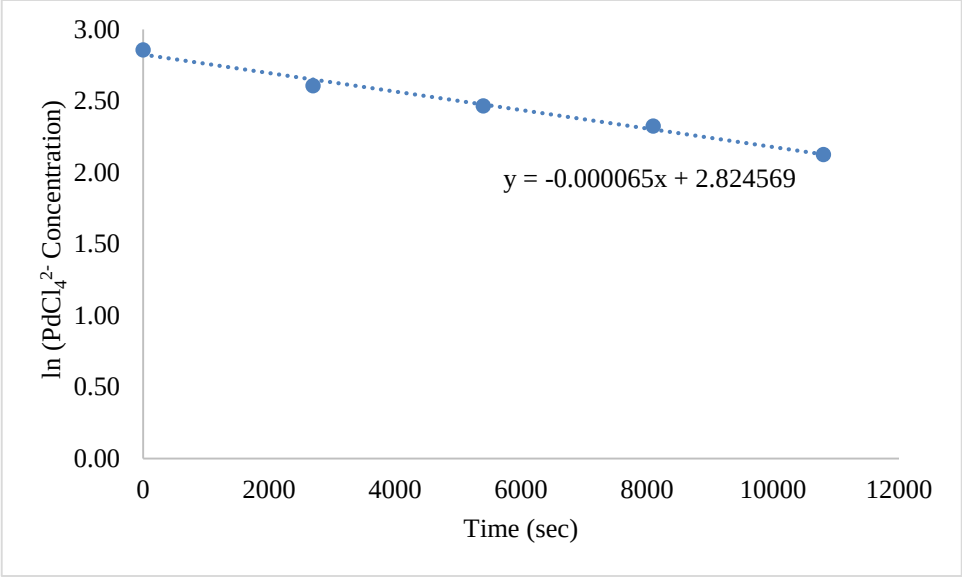

Figure 13: Natural logarithm of $PdCl_4^{2-}$ concentration versus time at different lengths of millifluidic reactor. A straight line is obtained with a slope of -k.

The data from Table 1 was used to plot Figure 13 to obtain straight line with slope of -k (rate constant of reaction). Based on obtained straight line, the rate constant of reaction is $6.5*10^{-5}$ s^{-1}.

The residue from each sample was washed using three cycles of centrifugation with deionized water in preparation for TEM. The TEM images at each length of the reactor demonstrated the nucleation phase of the reaction, followed by seed formation, and gradual growth of Pd nanorods. Figure 15 displays the evolution of the Pd nanostructures as the reaction solution passes through the 4 feet reactor.

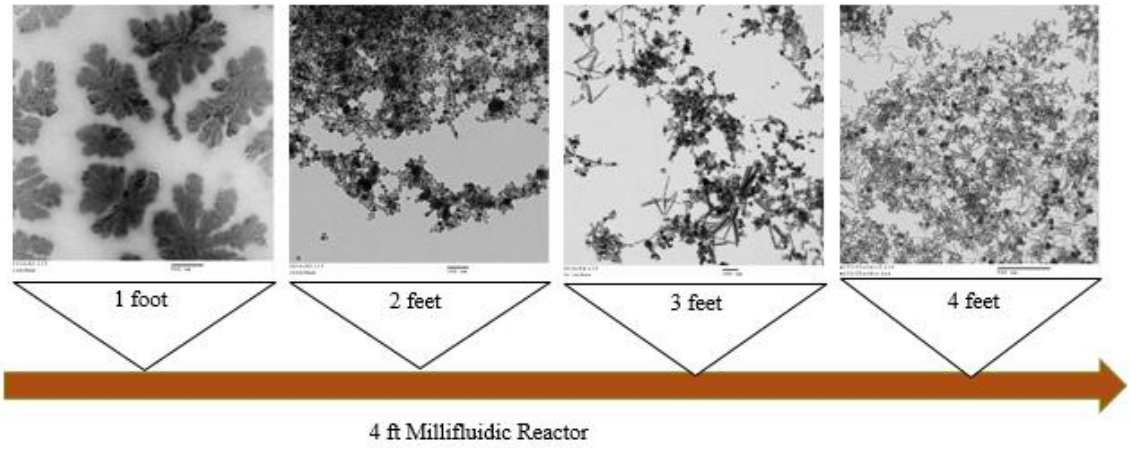

Figure 14: Evolution of Pd nanostructures as it flows through a specified length in the reactor.

Based on Figure 14, TEM images at 1 feet intervals display a series of interesting structures that could be a product of the initial nucleation that occurs in the reaction mechanism. These structures are drastically different from the synthesized Pd nanostructures; therefore, it may be hypothesized that the reduction reaction occurring in the early phase of the experiment is different from the precursor reduction occurring during rest of the reaction. An investigation on the reaction prior to the 1 foot mark on the reactor would uncover the nature of this reduction reaction. A separate kinetic study at shorter intervals less than 1 foot was performed to find how the reduction rate during initial nucleation compared with the rest of the reaction. At very short lengths, it is challenging to perform a millifluidic experiment. To overcome this challenge, the residence time corresponding to these lengths was simulated by altering flow rates. An experiment was designed with a 1foot millifluidic reactor, and various flow rates simulated residence times corresponding to 2 inches, 4 inches, 6, inches, 8 inches, 10 inches, and 12 inches. The $PdCl_4^{2-}$ ion concentration was determined using UV-Vis spectroscopy and the calibration curve. These results are summarized in Table 2.

Table 2: Absorbance at 425 nm, and corresponding $PdCl_4^{2-}$ concentration at different lengths of milllifluidic reactor before 1 feet mark.

Time (sec)	Length (inches)	Flow Rate (ml/min)	Absorbance at 425nm Wavelength	$[PdCl_4^{2-}]$ (mM)	ln $([PdCl_4^{2-}])$
2700	12	0.0067	0.32	13.55	2.61
2250	10	0.0080	0.33	13.93	2.63
1800	8	0.0101	0.35	15.09	2.71
1350	6	0.0134	0.39	16.48	2.80
900	4	0.0201	0.39	16.85	2.82
450	2	0.0402	0.41	17.37	2.85
0	0	0.0000	0.41	17.40	2.86

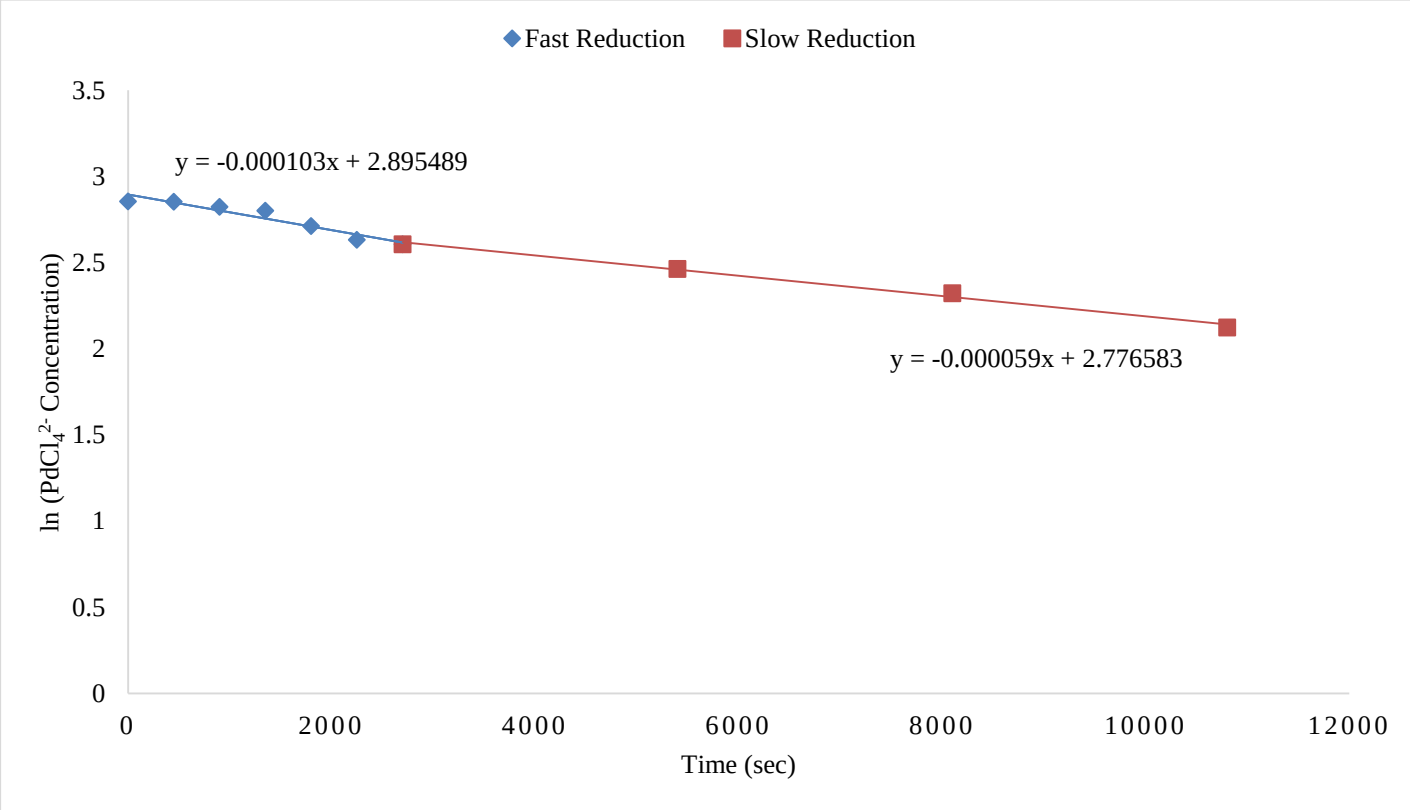

Figure 15: Natural logarithm of $PdCl_4^{2-}$ concentration versus time at different lengths of millifluidic reactor at two different sections.

Figure 15 demonstrates how the reduction rate varies at each stage of the millifluidic reactor. The analysis compares the reduction during first 1 foot of the reactor with rest of the reaction. In the first 1 foot of the reaction (45 minutes residence time), the rate constant of reaction (k) is $1.03*10^{-4}$ s^{-1} and $5.9*10^{-5}$ s^{-1} through the remainder of the reaction. This proves that reduction during initial stage of reaction is about 75% faster than during rest of the reaction. The slower reduction rate beyond 1 foot could be due to the increase in $PdBr_4^{2-}$ ions resulting from the ligand exchange reaction. Due to $PdBr_4^{2-}$ being more stable relative to $PdCl_4^{2-}$, they are reduced more slowly, resulting in a lower rate constant. It could be hypothesized that the high temperature in the oil bath promotes ligand exchange reaction, therefore over time $PdBr_4^{2-}$ ions concentration rises, leading to slower reduction rates. The UV-Vis data from figure 12 also provides some evidence, because the absorbance at 332 nm representing $PdBr_4^{2-}$ slightly increases from the spectrum for the 1foot reactor to the 2 feet one. There is a decline in 332 nm absorbance after 2 feet, demonstrating the gradual reduction of $PdBr_4^{2-}$ ions.

CHAPTER VII
RESULTS AND DISCUSSION – PD NANOROD SYNTHESIS USING VIRAL BIOTEMPLATES

Expression of TMV VLPs

TMV VLPs were expressed in *E. Coli* and stored in pH 7 phosphate buffer solution at 4 °C. The expressed TMV VLPs were examined using TEM to assess their quality. The lengths of the resulting TMV VLPs were measured from the TEM images and found to have an average length of about 350 nm.

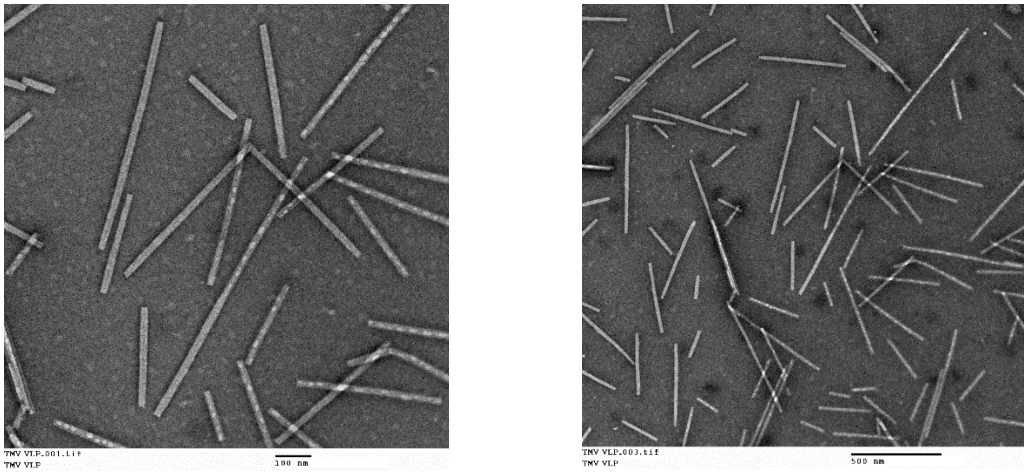

Figure 16: TEM images of TMV VLPs expressed in *E.coli* to be used as biotemplates for Pd mineralization.

Pd Nanorod Synthesis in a Batch Reactor at Baseline Conditions

Two baseline reaction conditions for the batch reactions were used, with both high and

low reagent concentrations, as both reaction conditions have been used in previous studies[114 115]. The ratio of TMV VLP concentration to Na_2PdCl_4 was maintained at 6.7. Na_2PdCl_4 concentrations of 0.25 mM and 2 mM were used. The effect of pH levels was studied by repeating reactions while maintaining pH level at 5 and without pH control. Experiments were also repeated at both room temperature and 50 °C to examine the effect of temperature on Pd mineralization.

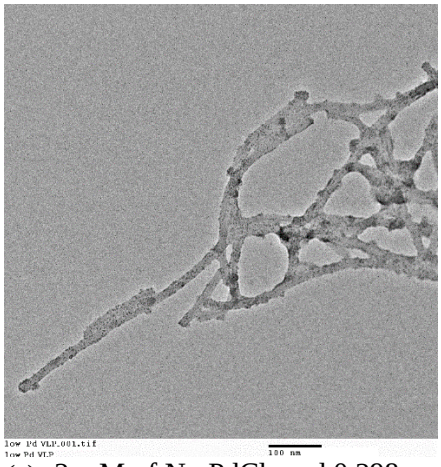

(a) 2 mM of Na_2PdCl_4 and 0.298 mg/ml TMV VLPs

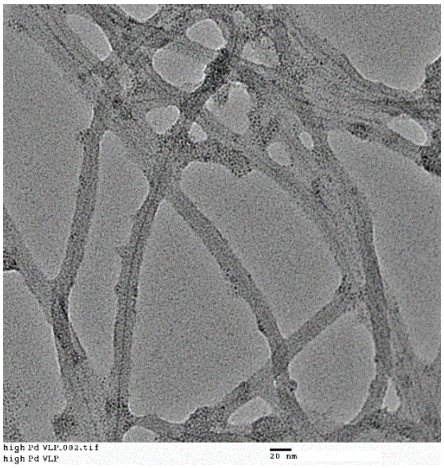

(b) 0.25 mM of Na_2PdCl_4 and 0.038 mg/ml TMV VLPs

Figure 17: Effect of (a) lower and (b) higher concentration of Na_2PdCl_4 and TMV VLPs on Pd mineralization on TMV VLPs.

Pd mineralization was observed on the surface of the TMV VLP virions as shown in Figure 18. The level of metal mineralization in each case was similar, but heavier aggregation was observed in the high concentration experiment. The similar degree of Pd mineralization can be due to ratio of Pd precursor to VLPs being kept constant. Greater concentration of reagents also resulted in denser virion aggregation producing a net-like complex of aggregated VLPs. Neither of the two experiments resulted in the synthesis of individual non-aggregated Pd mineralized TMV VLPs that are the product desired from Pd mineralization on rod-like virions.

Parametric Study of Pd Mineralization on TMV VLPs

Several parameters could affect Pd mineralization on TMV VLPs such as pH level, temperature and concentrations of Pd precursor and TMV VLPs. Each reaction parameter could be changed one at a time and the batch reaction could be carried out while keeping the other reaction conditions constant. The pH level could affect Pd deposition on the capsid protein of the virions because their isoelectric points determine the net charge on the external walls of the VLPs[32]. Generally, a pH of about 5 is preferable because it results in a net negative charge on the external walls of the virions, which is more conducive to Pd mineralization because metal ions are attracted to the negatively charged capsid protein walls. Temperature could potentially determine the level of Pd mineralization, because the rate of Pd ion reduction by the functional groups on the capsid protein surface could be affected by temperature. Higher temperatures could be hypothesized to result in higher rates of Pd precursor reduction, therefore facilitating high levels of metal mineralization. Pd mineralization on TMV virions have been observed even at low temperatures such as 4 °C in previous studies[115]. The ratio of concentrations of the two reagents would also determine the degree and uniformity of Pd mineralization on reacting virions. Based on previous studies, a Pd precursor to TMV ratio of 6.7 resulted in the most uniform metal mineralization on the virions[115]

Effect of pH Levels

The isoelectric point of the virions are found to be below a pH of about 5; therefore, if the pH level is greater, the coat protein will have a net negative charge that is more conducive to Pd mineralization[51]. This is due to the negatively charged capsid protein

attracting the Pd cations, and its effect can be studied by repeating the baseline experiment with pH adjusted to be just above 5. The VLP solution used in the experiment is stored in pH 7 buffer solution; therefore, the baseline experiment is performed under neutral pH conditions as no acid or alkaline was added to adjust the pH level. By adjusting the pH level close to the isoelectric point, the effect of pH on Pd mineralization could be observed.

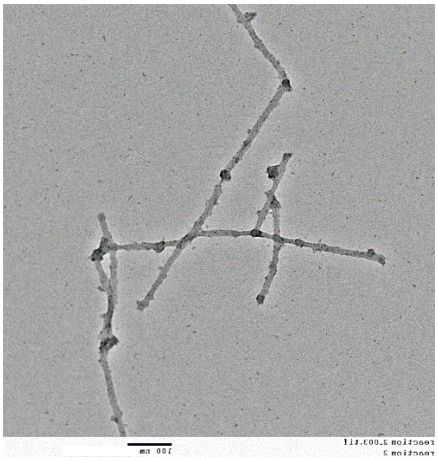

(a) 2 mM of Na_2PdCl_4 and 0.298 mg/ml TMV VLPs, pH of 5-5.5.

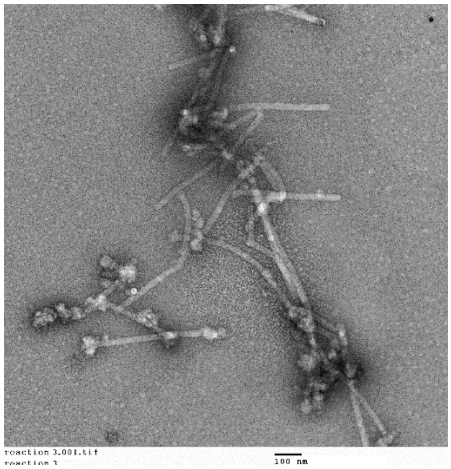

(b) 0.25 mM of Na_2PdCl_4 and 0.038 mg/ml TMV VLPs pH of 5-5.5.

Figure 18: Effect of pH control with (a) lower and (b) higher concentration of Na_2PdCl_4 and TMV VLPs on Pd mineralization on TMV VLPs.

When the pH level was monitored by a pH meter and maintained between 5 and 5.5 by adding hydrochloric acid, the samples resulted in the TEM images shown in Figure 18. In the high reagent concentration condition that used 0.5 mM Na_2PdCl_4 with pH control, no Pd mineralization was observed. The experiment with 2 mM Na_2PdCl_4 concentration resulted in virions with Pd mineralized in the form of knobs. This type of mineralization is not desirable because it does not result in uniform coating of the virions. Non-uniform deposition of Pd can be

due to lack of uniformity in the charge present on the TMV VLP coat protein at pH levels close to the isoelectric point.

Effect of Reagent Concentrations

Change in the ratio of Pd precursor to TMV VLP concentration also resulted in variations in Pd mineralization on TMV VLPs. Halving and doubling the of Pd precursor to TMV VLP concentration ratio would help to observe the influence of reagent concentration on Pd mineralization.

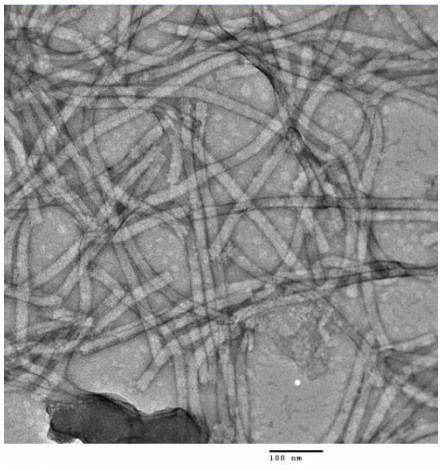

(a) 1 mM of Na_2PdCl_4 and 0.298 mg/ml TMV VLPs

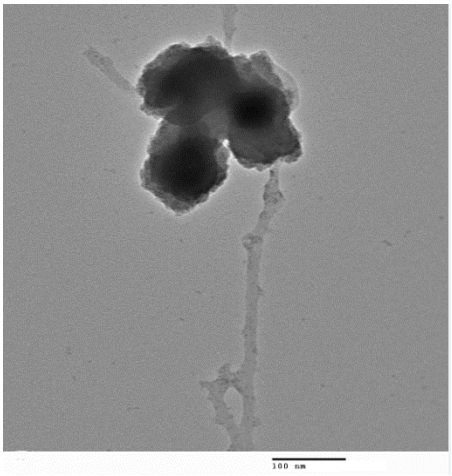

(b) 4 mM of Na_2PdCl_4 and 0.298 mg/ml TMV VLPs

Figure 19: Effect of Na_2PdCl_4 to TMV VLPs ratio of (a) 3.35 and (b) 13.40.

The ratio was doubled by doubling the concentration of Na_2PdCl_4, while the Pd precursor concentration was halved to get a lower precursor to virion concentration ratio. 0.298 mg/ml of TMV VLP concentration was used, as this was the parameter used in the baseline experiment with high concentration. Higher concentration of VLPs would make it more convenient to locate virions during TEM characterization. A Pd precursor to VLP ratio of 3.35 required 1 mM

Na_2PdCl_4 solution to be used, and at a 13.4 ratio 4 mM of Na_2PdCl_4 was used. Based on Figure 19, at high Pd precursor to VLP ratio, some of the mineralized Pd clumped onto a part of the virion, while there was uniform Pd mineralization on the rest of the VLP similar to the mineralization in the baseline condition. At low concentration ratio, no significant mineralization on the surface of the VLPs were observed as evident in figure 15. Based on the results, a minimum Pd precursor concentration is necessary for the metal mineralization to occur. Beyond the baseline precursor to TMV ratio no improved mineralization takes place, instead excess precursor mineralizes into metal clumps. This may be due to some of the capsid protein's amino acid residues (responsible for metal mineralization) being active at a given time[51]. Further investigation on capsid protein functional groups via a characterization technique such as FTIR would help understand the reduction of Pd ions on the virion surface.

CHAPTER VIII
CONCLUSION AND FUTURE DIRECTION

Pd Nanorod Synthesis Using Green Solvent and Reducing Agents

Pd nanorods were successfully synthesized using L-ascorbic acid as a green reducing agent, PVP as stabilizer, and KBr as the capping agent. Other nanostructures such as nanocubes, nanobars, and multiple-twinned structures were also synthesized alongside Pd nanorods. Multiple-twinned structure decahedrons are the seeds that develop into five-fold Pd nanorods; therefore, their formation needs to be maximized. To produce more multiple-twinned seed structures, the synthesis process should be thermodynamically controlled that can be achieved by adjusting reduction rate. This relatively higher reduction rates are favorable for thermodynamically controlled process; however, extremely high reduction rate may also results in single crystal seed structures that are not desirable for 1D Pd nanorod synthesis. Results illustrated that L-ascorbic acid with relatively high reducing power alongside with Br^- ions that would form complex, release Pd ions slowly, and consequently adjust the reducing power is favorable for controlling the type of initially formed seeds and corresponding synthesized Pd nanostructures. Restricting oxidative etching by minimizing presence of air in the reaction mixture through the use of a continuous-flow millifluidic reactor resulted in a greater proportion of twinned structures such as decahedrons during nucleation. These seeds would then undergo 1D growth in the presence of KBr that preferentially absorbs on {100} facet of the seeds and facilitates the longitudinal growth that resulted in more Pd nanorods being produced. The compartmentalized flow of the reaction

solution caused by the boiling point reaction temperature also improved the reaction through better mixing and heat transfer.

In the parametric study, the effect of variation in reactant concentrations were studied. Higher ascorbic acid concentrations led to faster reduction rates; therefore, resulting in more multiple-twinned structures being produced but the faster reduction prevented the slow release of Pd atoms resulting from the Pd salt reduction that is necessary for 1D growth; therefore, resulting in fewer nanorods. At lower reducing agent concentrations, the rate of reduction is too low for multiple-twinned structure production that also resulted in fewer nanorods. High KBr concentrations led to more oxidative etching during nanorod growth and discouraging the synthesis of 1D nanostructures. At low KBr concentrations, there is relatively less ligand exchange taking place to form the relatively more stable $PdBr_4^{2-}$ ions; therefore, the reduction rate is too fast for 1D growth and resulted in fewer Pd nanorods. High stabilizer concentration resulted in no change from the baseline results that means excess PVP in the reaction solution has no effect on nanostructure synthesis. Low stabilizer concentration resulted in fewer nanorods due to lack of sufficient PVP present to stabilize the surface of decahedron seeds.

The kinetic study discovered the reduction rate at which the Pd nanorods were synthesized and a separate kinetic study was also conducted on the first 1 foot of the millifluidic reactor to observe the early phase of the reaction. As expected, the initial reduction rate was about 75% faster compared to the rest of the reaction. The initially higher reduction rate contributes to greater multiple-twinned structure synthesis; therefore, more decahedron seeds will be available for 1D growth. The relatively slower reduction rate after 1 foot is helpful for Pd nanorod production because the slow release of Pd atoms from Na_2PdCl_4 reduction promotes facet growth. The lowering of reduction rates as time passes can be due to the formation of stable $PdBr_4^{2-}$ complex that slows down the reaction.

For future studies, further investigation on Pd nanorod synthesis using L-ascorbic acid needs to be conducted by performing the kinetic study at different reaction conditions. The effect of temperature on the reduction rate should be examined by performing the kinetic study at different temperatures. However, the compartmentalized plug flow observed at boiling point might not be possible at lower temperatures, and the effect of change in reaction temperature on reduction rates should be analyzed while paying attention to this fact. The change in concentration of reducing agent could also be altered in the kinetic study to understand how its concentration correlates with the rate of reduction and concentration of multiple twinned seeds. TEM characterization need to be employed to investigate how the type of seeds and their concentration and consequent size, structure, and morphology of the synthesized Pd nanorods correlate with the rate of reduction. The final goal should be finding the rate of reduction rates at which concentration of multiple twinned seeds and corresponding five-fold nanorod are maximized.

The novel proposed multifluidic system is adaptable for *in-situ* monitoring characterizations. Novel *in-situ* characterization techniques are essential for reaction mechanism investigation to control the morphology of the synthesized 1D Pd nanostructures. *In-situ* X-ray absorption spectroscopy (XAS) is a versatile technique that provides an opportunity to investigate the reaction dynamic and mechanism of 1D Pd nanostructure growth in millifluidic reactor specifically during the nucleation and initial nuclei and seed formation to further control their morphology, size distribution, and crystal structures. The future study may focus to determine state of the palladium as it reduces, nucleates, and grow through the course of millifluidic synthesis by *in-situ* XAS studies at different positions of the millifluidic tubular reactor. Moreover, the Artificial Neural Network (ANN) tools may also be applied in millifluidic synthesis of Pd nanorod that would prime to save time and expenditure by predicting the reactions' outcomes in which the most desirable nanomaterial size and morphology is achieved.

Finally, further investigating needs to be done for optimized large-scale industrial relevant production by either scaling up or numbering up of millifluidic reactors.

Pd Nanorod Synthesis Using Viral Biotemplates

The experiments demonstrated that TMV VLPs Pd mineralization on TMV VLPs was observed to be uniform under neutral pH, a Pd precursor to TMV VLPs concentration ratio of 6.7, and 50 °C in the dark as found in previous studies[32]. However, the virions aggregated into a net of virions. Variations in reaction parameters such as the pH level, the ratio of Pd precursor to TMV VLPs concentration ratio, and concentration of the reagents did not prevent aggregation. The high concentration reactions resulted in higher density of virions in the net of aggregated virions. Lowering of the pH levels resulted in the formation of Pd clumps on the VLP surface; thus, resulting in uneven coating of the virion. Increasing the ratio of Pd precursor to TMV VLPs concentration resulted in excess Pd mineralization, and reduction in the ratio also resulted in reduction in the Pd coating on the virions.

For future study, additional approaches need to be used to improve Pd mineralization on TMV VLPs, and this includes the use of continuous-flow reactors. Continuous-flow reactors can be used to attain more control over the material transport of the reactants, thereby optimizing Pd mineralization on TMV VLP virions. A continuous-flow reactor may potentially prevent aggregation of virions during Pd mineralization. The reaction occurs in a small volume within millifluidic or microfluidic tubing relative to a batch reactor therefore the VLPs are less likely to aggregate. This could result in individual virions with Pd mineralized on them without aggregating into lumps. Better control over material transport of reactants available in continuous flow reactors may be utilized for better mixing of reactant; thereby, promoting more uniform Pd

deposition on the surface of the virions. Fewer cycles of coating might also be needed to produce fully coated virion nanorods due to improved coating of Pd on TMV VLPs via millifluidic reactors. The reaction conditions resulting in the most uniform Pd deposition on TMV VLPs with least amounts of aggregation in the batch experiments may be repeated in a continuous-flow reactor. A millifluidic reactor is more suitable than a microfluidic reactor for the experiment due to the ease of building a millifluidic reactor with the material available in a laboratory.

The activity of the functional groups present on TMV VLP capsid protein during Pd mineralization will help to describe the mechanism of the Pd ion reduction and Pd nanoparticle formation on the surface of the virions. The vibrations of the capsid protein functional groups active in precursor reduction can be detected using Fourier-Transform Infrared (FTIR spectroscopy). An *in-situ* FTIR characterization of the reaction would help to identify the functional groups of amino acids on the surface of coat proteins involved in Pd ions reduction as a function of time. As the data is collected in real time, the different functional groups active at different stages of Pd mineralization can be recognized. Based on the findings from *in-situ* FTIR characterization, other amino acid residues apart from cysteine may be added as modifications to the virions to improve Pd mineralization. *In-situ* UV-vis analysis may also be used to find the reduction rate and rate constant at the beginning of the reaction to realize what is the range of reduction rate hypothetically depending on reaction parameters such as temperature, pH, and concentration ratio that maximize the smoothness and coverage of Pd on TMV VLP.

Metallic nanomaterials are frequently sought out for nanoelectronics applications such as transparent conductive films (TCFs) and require high electrical conductivity to carry an electrical current. The mechanism of Pd deposition on template creates grain boundaries or an uneven surface that impedes electron/energy transport resulting in low electrical conductivities. Thermal annealing is a common metal processing technology to alter the material crystal structure, removing grain boundaries, and improving the material's transport and physical properties. So, it

is essential to optimal annealing process to remove biotemplate and produce single crystal Pd nanorods.

REFERENCES

1. Lee, K. Z. *et al.* Engineering Tobacco Mosaic Virus and Its Virus-Like-Particles for Synthesis of Biotemplated Nanomaterials. *Biotechnology Journal* (2020)

2. Huang, H. *et al.* One-Pot Synthesis of Penta-twinned Palladium Nanowires and Their Enhanced Electrocatalytic Properties. *ACS Appl. Mater. Interfaces* **9**, 31203–31212 (2017).

3. Köhler, J. M., Li, S. & Knauer, A. Why is Micro Segmented Flow Particularly Promising for the Synthesis of Nanomaterials? *Chem. Eng. Technol.* **36**, 887–899 (2013).

4. Andersen, O. K. Electronic structure of the fcc transition metals Ir, Rh, Pt, and Pd. *Phys. Rev. B* **2**, 883–906 (1970).

5. Wei, C., Antolin, N., Restrepo, O. D., Windl, W. & Zhao, J. C. A general model for thermal and electrical conductivity of binary metallic systems. *Acta Mater.* **126**, 272–279 (2017).

6. Taylor, K. C. Automobile catalytic converters. in *Studies in Surface Science and Catalysis* vol. 30 97–116 (1987).

7. Nadagouda, M. N. & Varma, R. S. Green Synthesis of Ag and Pd Nanospheres, Nanowires, and Nanorods Using Vitamin Catalytic Polymerisation of Aniline and Pyrrole. *J. Nanomater.* **2008**, 1–8 (2008).

8. Murphy, Controlling the Aspect Ratio of Inorganic Nanorods and Nanowires. Advanced Materials. Wiley Online Library (2002).

9. Chen, Y. H., Hung, H. H. & Huang, M. H. Seed-mediated synthesis of palladium nanorods and branched nanocrystals and their use as recyclable suzuki coupling reaction catalysts. *J. Am. Chem. Soc.* **131**, 9114–9121 (2009).

10. Lee, Y. C., Huang, H., Tan, O. K. & Tse, M. S. Semiconductor gas sensor based on Pd-doped SnO2 nanorod thin films. *Sensors Actuators, B Chem.* **132**, 239–242 (2008).

11. Rodal-Cedeira, S. *et al.* Plasmonic Au@Pd Nanorods with Boosted Refractive Index Susceptibility and SERS Efficiency: A Multifunctional Platform for Hydrogen Sensing and Monitoring of Catalytic Reactions. *Chem. Mater.* **28**, 9169–9180 (2016).

12. Xiao, C. *et al.* Shape-controlled synthesis of palladium nanorods and their magnetic properties. *J. Phys. Chem. C* **113**, 13466–13469 (2009).

13. Liu, B. *et al.* Interfacial Effects of CeO2-Supported Pd Nanorod in Catalytic CO Oxidation: A Theoretical Study. *J. Phys. Chem. C* **119**, 12923–12934 (2015).

14. Zhang, H., Jin, M., Xiong, Y., Lim, B. & Xia, Y. Shape-controlled synthesis of Pd nanocrystals and their catalytic applications. *Acc. Chem. Res.* **46**, 1783–1794 (2013).

15. Qu, F., Sun, H., Zhang, Y., Lu, H. & Yang, M. Electrochemically deposited Pd nanorod array/sol-gel silica thin film for the fabrication of electrochemical sensors. *Sensors Actuators, B Chem.* **166**–**167**, 837–841 (2012).

16. Wang, Y. *et al.* Polyol Synthesis of Ultrathin Pd Nanowires via Attachment-Based Growth and Their Enhanced Activity towards Formic Acid Oxidation. *Adv. Funct. Mater.* **24**, 131–139 (2014).

17. Chen, F., Zhong, Z., Xu, X.-J. & Luo, J. *Preparation of colloidal Pd nanoparticles by an ethanolamine-modified polyol process* (2005).

18. Lee, S.-Y. *et al.* Deposition of platinum clusters on surface-modified tobacco mosaic virus. *J. Nanosci. Nanotechnol.* **4**, 974–981 (2006).

19. Toxicology, N. R. C. (US) C. on. ETHANOLAMINE. (1984).

20. Schep, L. J., Slaughter, R. J., Temple, W. A. & Beasley, D. M. G. Diethylene glycol poisoning. *Clinical Toxicology* vol. 47 525–535 (2009).

21. Pekkari, A. *et al.* Continuous Microfluidic Synthesis of Pd Nanocubes and PdPt Core-Shell Nanoparticles and Their Catalysis of NO2 Reduction. *ACS Appl. Mater. Interfaces* **11**, 36196–36204 (2019).

22. Yoshida, J. I., Nagaki, A. & Yamada, D. Continuous flow synthesis. *Drug Discovery Today: Technologies* vol. 10 e53–e59 (2013).

23. Roberts, E. J., Karadaghi, L. R., Wang, L., Malmstadt, N. & Brutchey, R. L. Continuous Flow Methods of Fabricating Catalytically Active Metal Nanoparticles. *ACS Applied Materials and Interfaces* vol. 11 27479–27502 (2019).

24. Kockmann, N., Gottsponer, M. & Roberge, D. M. Scale-up concept of single-channel microreactors from process development to industrial production. *Chem. Eng. J.* **167**, 718–726 (2011).

25. Niu, G., Ruditskiy, A., Vara, M. & Xia, Y. Toward continuous and scalable production of colloidal nanocrystals by switching from batch to droplet reactors. *Chem. Soc. Rev.* **44**, 5806–5820 (2015).

26. Yue, H., Zhao, Y., Ma, X. & Gong, J. Ethylene glycol: Properties, synthesis, and applications. *Chem. Soc. Rev.* **41**, 4218–4244 (2012).

27. Bankar, A., Joshi, B., Kumar, A. R. & Zinjarde, S. Banana peel extract mediated novel route for the synthesis of palladium nanoparticles. *Mater. Lett.* **64**, 1951–1953 (2010).

28. Arsiya, F., Sayadi, M. H. & Sobhani, S. Green synthesis of palladium nanoparticles using Chlorella vulgaris. (2016).

29. Lim, B. *et al.* Shape-Controlled Synthesis of Pd Nanocrystals in Aqueous Solutions (2013).

30. Xiong, Y., Cai, H., Yin, Y. & Xia, Y. Synthesis and characterization of fivefold twinned

nanorods and right bipyramids of palladium (2007).

31. Nadagouda, M. N. & Varma, R. S. Green and controlled synthesis of gold and platinum nanomaterials using vitamin B 2 : density-assisted self-assembly of nanospheres, wires and rods (2006).

32. Adigun, O. O. *et al.* BSMV as a Biotemplate for Palladium Nanomaterial Synthesis. *Langmuir* **33**, 1716–1724 (2017).

33. Santoshi, A., Maragoni, •, Dasari, V. •, • A. & Veerabhadram, G. Green synthesis, characterization and catalytic activity of palladium nanoparticles by xanthan gum (2014).

34. SU Yuanbo,LI Qingbiao,YAO Chuanyi,LU Yinghua, H. J. Antitumor action of ethanolic extractives from camphor leaves (2006).

35. Momeni, S. & Nabipour, I. A Simple Green Synthesis of Palladium Nanoparticles with Sargassum Alga and Their Electrocatalytic Activities Towards Hydrogen Peroxide. *Appl. Biochem. Biotechnol.* **176**, 1937–1949 (2015).

36. Prasad, B. S. N. & Padmesh, T. N. Seaweed (Sargassum ilicifolium) assisted green synthesis of palladium nanoparticles. (2014).

37. Veisi, H., Faraji, A. R., Hemmati, S. & Gil, A. Green synthesis of palladium nanoparticles using *Pistacia atlantica kurdica* gum and their catalytic performance in Mizoroki-Heck and Suzuki-Miyaura coupling reactions in aqueous solutions. *Appl. Organomet. Chem.* **29**, 517–523 (2015).

38. Sheny, D. S., Philip, D. & Mathew, J. Spectrochimica Acta Part A: Molecular and Biomolecular Spectroscopy Rapid green synthesis of palladium nanoparticles using the dried leaf of Anacardium occidentale. *Spectrochim. Acta Part A* **91**, 35–38 (2012).

39. Yue, J., Du, Z. & Shao, M. The role of citric acid and ascorbic acid in morphology control of palladium nanocrystals: A molecular dynamics and density functional theory study. (2016).

40. Azizi, S. *et al.* Green synthesis palladium nanoparticles mediated by white tea (Camellia sinensis) extract with antioxidant, antibacterial, and antiproliferative activities toward the human leukemia (MOLT-4) cell line. *Int. J. Nanomedicine* **12**, 8841–8853 (2017).

41. Sathishkumar, M. *et al.* Phyto-crystallization of palladium through reduction process using Cinnamom zeylanicum bark extract. *J. Hazard. Mater.* **171**, 400–404 (2009).

42. Kumar, K. M., Kumar Mandal, B., Siva Kumar, K., Sreedhara Reddy, P. & Sreedhar, B. Biobased green method to synthesise palladium and iron nanoparticles using Terminalia chebula aqueous extract Spectrochimica Acta Part A: Molecular and Biomolecular Spectroscopy. *Spectrochim. Acta Part A Mol. Biomol. Spectrosc.* **102**, 128–133 (2013).

43. Kumar Petla, R., Vivekanandhan, S., Misra, M., Kumar Mohanty, A. & Satyanarayana, N. Soybean (<i>Glycine Max</i>) Leaf Extract Based Green Synthesis of Palladium Nanoparticles. *J. Biomater. Nanobiotechnol.* **03**, 14–19 (2012).

44. Strachan, J. Solubility of cellulose in water [11]. *Nature* vol. 141 332–333 (1938).

45. He, F. & Zhao, D. Manipulating the size and dispersibility of zerovalent iron nanoparticles

by use of carboxymethyl cellulose stabilizers. *Environ. Sci. Technol.* **41**, 6216–6221 (2007).

46. Camp, J. E. *et al.* Recyclable glucose-derived palladium(0) nanoparticles as in situ-formed catalysts for cross-coupling reactions in aqueous media. *RSC Adv.* **6**, 16115–16121 (2016).

47. Hemmati, S., Retzlaff-Roberts, E., Scott, C. & Harris, M. T. Research Article Artificial Sweeteners and Sugar Ingredients as Reducing Agent for Green Synthesis of Silver Nanoparticles. (2019).

48. Cushing, B. L., Kolesnichenko, V. L. & O'connor, C. J. Recent Advances in the Liquid-Phase Syntheses of Inorganic Nanoparticles (2004).

49. Manikandan, V. *et al.* Synthesis and antimicrobial activity of palladium nanoparticles from Prunus × yedoensis leaf extract. *Mater. Lett.* **185**, 335–338 (2016).

50. Surendra, T. V., Roopan, S. M., Arasu, M. V., Al-Dhabi, N. A. & Rayalu, G. M. RSM optimized Moringa oleifera peel extract for green synthesis of M. oleifera capped palladium nanoparticles with antibacterial and hemolytic property. *J. Photochem. Photobiol. B Biol.* **162**, 550–557 (2016).

51. Improved metal cluster deposition on a genetically engineered tobacco mosaic virus template Related content. (2005).

52. Huang, H. *et al.* One-Pot Synthesis of Penta-twinned Palladium Nanowires and Their Enhanced Electrocatalytic Properties. *ACS Appl. Mater. Interfaces* **9**, 31203–31212 (2017).

53. Ma, N. *et al.* Carrageenan Asissted Synthesis of Palladium Nanoflowers and Their Electrocatalytic Activity toward Ethanol. *ACS Sustain. Chem. Eng.* **6**, 1133–1140 (2018).

54. Nadagouda, M. N., Polshettiwar, V. & Varma, R. S. Self-assembly of palladium nanoparticles: Synthesis of nanobelts, nanoplates and nanotrees using vitamin B1, and their application in carbon-carbon coupling reactions. *J. Mater. Chem.* **19**, 2026–2031 (2009).

55. Fu, G. *et al.* Green synthesis and catalytic properties of polyallylamine functionalized tetrahedral palladium nanocrystals. *Appl. Catal. B Environ.* **138**–**139**, 167–174 (2013).

56. Powell, A. W. *et al.* Plasmonic Gas Sensing Using Nanocube Patch Antennas. *Adv. Opt. Mater.* **4**, 634–642 (2016).

57. Maciel, M. V. de O. B. *et al.* <i> Syzygium aromaticum</i> L. (Clove) Essential Oil as a Reducing Agent for the Green Synthesis of Silver Nanoparticles. *Open J. Appl. Sci.* **09**, 45–54 (2019).

58. Xiong, Y. & Xia, Y. Shape-Controlled Synthesis of Metal Nanostructures: The Case of Palladium. *Adv. Mater.* **19**, 3385–3391 (2007).

59. Yang, T.-H., Gilroy, K. D. & Xia, Y. Reduction rate as a quantitative knob for achieving deterministic synthesis of colloidal metal nanocrystals. (2017).

60. Xiong, Y., Huang, L., Mahmud, S., Yang, F. & Liu, H. Bio-synthesized palladium nanoparticles using alginate for catalytic degradation of azo-dyes. *Chinese J. Chem. Eng.*

28, 1334–1343 (2020).

61. Sathishkumar, M. *et al.* Phyto-crystallization of palladium through reduction process using Cinnamom zeylanicum bark extract. *J. Hazard. Mater.* **171**, 400–404 (2009).

62. Qingbiao, Y., Li et al. Green synthesis of palladium nanoparticles using broth of Cinnamomum camphora leaf (2008).

63. Narayanan, R. & El-Sayed, M. A. Catalysis with transition metal nanoparticles in colloidal solution: Nanoparticle shape dependence and stability. *J. Phys. Chem. B* **109**, 12663–12676 (2005).

64. Siddiqi, K. S. & Husen, A. Green Synthesis, Characterization and Uses of Palladium/Platinum Nanoparticles. *Nanoscale Research Letters* vol. 11 1–13 (2016).

65. Basavegowda, N., Mishra, K. & Lee, Y. R. Ultrasonic-assisted green synthesis of palladium nanoparticles and their nanocatalytic application in multicomponent reaction. *New J. Chem.* **39**, 972–977 (2015).

66. Kim, Y. H. *et al.* Droplet-Based Microreactors for Continuous Production of Palladium Nanocrystals with Controlled Sizes and Shapes. *Small* **9**, 3462–3467 (2013).

67. Zhang, L. *et al.* Continuous and scalable production of well-controlled noble-metal nanocrystals in milliliter-sized droplet reactors. *Nano Lett.* **14**, 6626–6631 (2014).

68. Niu, G., Zhang, L., Ruditskiy, A., Wang, L. & Xia, Y. A Droplet-Reactor System Capable of Automation for the Continuous and Scalable Production of Noble-Metal Nanocrystals. *Nano Lett.* **18**, 3879–3884 (2018).

69. Sebastian, V., Basak, S. & Jensen, K. F. Continuous synthesis of palladium nanorods in oxidative segmented flow. *AIChE J.* **62**, 373–380 (2016).

70. PALLADIUM CATALYSTS. *Org. Synth.* **26**, 77 (1946).

71. ATSDR - Medical Management Guidelines (MMGs): Formaldehyde (2020).

72. haynes, H. W. Effect of particle size distribution on catalyst effectiveness. *J. Catal.* **79**, 470–474 (1983).

73. Khazaei, M., Khazaei, A., Nasrollahzadeh, M. & Tahsili, M. R. Highly efficient reusable Pd nanoparticles based on eggshell: Green synthesis, characterization and their application in catalytic reduction of variety of organic dyes and ligand-free oxidative hydroxylation of phenylboronic acid at room temperature. *Tetrahedron* **73**, 5613–5623 (2017).

74. Anjana, P. M., Bindhu, M. R., Umadevi, M. & Rakhi, R. B. Antibacterial and electrochemical activities of silver, gold, and palladium nanoparticles dispersed amorphous carbon composites. *Appl. Surf. Sci.* **479**, 96–104 (2019).

75. Mohamed, M. A., Fekry, A. M., El-Shal, M. A. & Banks, C. E. Incorporation of Tetrazolium Blue (TB)/Gold Nanoparticles (GNPs) into Carbon Paste Electrode: Application as an Electrochemical Sensor for the Sensitive and Selective Determination of Sotalol in Micellar Medium. *Electroanalysis* **29**, 2551–2558 (2017).

76. Wang, H., Yuan, Y., Chai, Y. & Yuan, R. Self-enhanced electrochemiluminescence

immunosensor based on nanowires obtained by a green approach. *Biosens. Bioelectron.* **68**, 72–77 (2015).

77. Chen, Z., Liu, Y., Wang, Y., Zhao, X. & Li, J. Dynamic evaluation of cell surface N-glycan expression via an electrogenerated chemiluminescence biosensor based on concanavalin A-integrating gold-nanoparticle-modified Ru(bpy)32+-doped silica nanoprobe. *Anal. Chem.* **85**, 4431–4438 (2013).

78. Nasrollahzadeh, M., Sajadi, S. M. & Maham, M. Green synthesis of palladium nanoparticles using Hippophae rhamnoides Linn leaf extract and their catalytic activity for the Suzuki-Miyaura coupling in water. *J. Mol. Catal. A Chem.* **396**, 297–303 (2015).

79. Thangavel, S., Dash, K., Thangavel, S., Chaurasia, S. C. & Arunachalam, J. *Determination of Mercury in Hepatitis-B Vaccine by Electrothermal Atomic Absorption Spectrometry (ETAAS) Using Colloidal Palladium as Modifier*. *Atomic Spectroscopy* vol. 30 (2009).

80. Ameri, A. *et al.* Rapid and Facile Microwave-Assisted Synthesis of Palladium Nanoparticles and Evaluation of Their Antioxidant Properties and Cytotoxic Effects Against Fibroblast-Like (HSkMC) and Human Lung Carcinoma (A549) Cell Lines. *Biol. Trace Elem. Res.* **197**, 132–140 (2020).

81. Mohana, S. & Sumathi, S. Multi-Functional Biological Effects of Palladium Nanoparticles Synthesized Using Agaricus bisporus. *J. Clust. Sci.* **31**, 391–400 (2020).

82. Gurunathan, S., Kim, E., Han, J., Park, J. & Kim, J.-H. Green Chemistry Approach for Synthesis of Effective Anticancer Palladium Nanoparticles. *Molecules* **20**, 22476–22498 (2015).

83. Azizi, S. *et al.* Green synthesis palladium nanoparticles mediated by white tea (Camellia sinensis) extract with antioxidant, antibacterial, and antiproliferative activities toward the human leukemia (MOLT-4) cell line. *Int. J. Nanomedicine* **12**, 8841–8853 (2017).

84. Vijilvani, C. *et al.* Antimicrobial and catalytic activities of biosynthesized gold, silver and palladium nanoparticles from Solanum nigurum leaves. *J. Photochem. Photobiol. B Biol.* **202**, 111713 (2020).

85. Anand, K. *et al.* Biosynthesis of palladium nanoparticles by using Moringa oleifera flower extract and their catalytic and biological properties. *J. Photochem. Photobiol. B Biol.* **165**, 87–95 (2016).

86. Collmer, C. W., Vogt, V. M. & Zaitlin, M. H protein, a minor protein of TMV virions, contains sequences of the viral coat protein. *Virology* **126**, 429–48 (1983).

87. Clare, D. K. *et al.* Novel inter-subunit contacts in barley stripe mosaic virus revealed by cryo-electron microscopy. *Structure* **23**, 1815–1826 (2015).

88. Makarov, V. V. *et al.* Structural Lability of Barley Stripe Mosaic Virus Virions. *PLoS One* **8**, 1–9 (2013).

89. Fan, X. Z. *et al.* Integration of genetically modified virus-like-particles with an optical resonator for selective bio-detection. *Nanotechnology* **26**, (2015).

90. Malm, M., Tamminen, K., Lappalainen, S., Vesikari, T. & Blazevic, V. Rotavirus

Recombinant VP6 Nanotubes Act as an Immunomodulator and Delivery Vehicle for Norovirus Virus-Like Particles. *J. Immunol. Res.* **2016**, (2016).

91. Dawson, W. O., Schlegel, D. E. & Lung, M. C. Y. Synthesis of tobacco mosaic virus in intact tobacco leaves systemically inoculated by differential temperature treatment. *Virology* **65**, 565–573 (1975).

92. Colby, L. A., Quenee, L. E. & Zitzow, L. A. Considerations for infectious disease research studies using animals. *Comp. Med.* **67**, 222–231 (2017).

93. Khan, A. A. *et al.* pH Control of the Electrostatic Binding of Gold and Iron Oxide Nanoparticles to Tobacco Mosaic Virus. *Langmuir* **29**, 2094–2098 (2013).

94. Kobayashi, M. *et al.* Chiral meta-molecules consisting of gold nanoparticles and genetically engineered tobacco mosaic virus. *Opt. Express* **20**, 24856 (2012).

95. Royston, E. S., Brown, A. D., Harris, M. T. & Culver, J. N. Preparation of silica stabilized Tobacco mosaic virus templates for the production of metal and layered nanoparticles. *J. Colloid Interface Sci.* **332**, 402–407 (2009).

96. Dujardin, E., Peet, C., Stubbs, G., Culver, J. N. & Mann, S. Organization of Metallic Nanoparticles Using Tobacco Mosaic Virus Templates. *Nano Lett.* **3**, 413–417 (2003).

97. Lim, J.-S. *et al.* Biotemplated Aqueous-Phase Palladium Crystallization in the Absence of External Reducing Agents. *Nano Lett.* **10**, 3863–3867 (2010).

98. Manocchi, A. K., Seifert, S., Lee, B. & Yi, H. In Situ Small-Angle X-ray Scattering Analysis of Palladium Nanoparticle Growth on Tobacco Mosaic Virus Nanotemplates. *Langmuir* **27**, 7052–7058 (2011).

99. Zhou, J. C. *et al.* Biotemplating rod-like viruses for the synthesis of copper nanorods and nanowires. *J. Nanobiotechnology* **10**, 18 (2012).

100. Royston, E., Ghosh, A., Kofinas, P., Harris, M. T. & Culver, J. N. Self-assembly of virus-structured high surface area nanomaterials and their application as battery electrodes. *Langmuir* **24**, 906–912 (2008).

101. Knez, M. *et al.* Biotemplate Synthesis of 3-nm Nickel and Cobalt Nanowires. *Nano Lett.* **3**, 1079–1082 (2003).

102. Balci, S. *et al.* Electroless synthesis of 3nm wide alloy nanowires inside Tobacco mosaic virus. *Nanotechnology* **23**, (2012).

103. Tsukamoto, R., Muraoka, M., Seki, M., Tabata, H. & Yamashita, I. Synthesis of CoPt and $FePt_3$ Nanowires Using the Central Channel of Tobacco Mosaic Virus as a Biotemplate. *Chem. Mater.* **19**, 2389–2391 (2007).

104. Wnęk, M. *et al.* Fabrication and characterization of gold nano-wires templated on virus-like arrays of tobacco mosaic virus coat proteins. *Nanotechnology* **24**, (2013).

105. Xiong, Y., Cai, H., Yin, Y. & Xia, Y. Synthesis and characterization of fivefold twinned nanorods and right bipyramids of palladium. *Chem. Phys. Lett.* **440**, 273–278 (2007).

106. Huo, D. *et al.* One-Dimensional Metal Nanostructures: From Colloidal Syntheses to

Applications. *Chemical Reviews* vol. 119 8972–9073 (2019).

107. Xiong, Y., Cai, H., Yin, Y. & Xia, Y. Synthesis and characterization of fivefold twinned nanorods and right bipyramids of palladium. *Chem. Phys. Lett.* **440**, 273–278 (2007).

108. Wang, Y. *et al.* Shape-controlled synthesis of palladium nanocrystals: A mechanistic understanding of the evolution from octahedrons to tetrahedrons. *Nano Lett.* **13**, 2276–2281 (2013).

109. Zheng, Y., Zeng, J., Ruditskiy, A., Liu, M. & Xia, Y. Oxidative etching and its role in manipulating the nucleation and growth of noble-metal nanocrystals. *Chemistry of Materials* vol. 26 22–33 (2014).

110. Koczkur, K. M., Mourdikoudis, S., Polavarapu, L. & Skrabalak, S. E. Polyvinylpyrrolidone (PVP) in nanoparticle synthesis. *Dalt. Trans.* **44**, 17883–17905 (2015).

111. Feng, H. *et al.* Multilayered Pd nanocatalysts with nano-bulge structure in a microreactor for multiphase catalytic reaction. *Chem. Eng. Res. Des.* **138**, 190–199 (2018).

112. Figueroa-Cosme, L. *et al.* Synthesis of Palladium Nanoscale Octahedra through a One-Pot, Dual-Reductant Route and Kinetic Analysis. *Chem. - A Eur. J.* **24**, 6133–6139 (2018).

113. Xie, M. *et al.* A Quantitative Analysis of the Reduction Kinetics Involved in the Synthesis of Au@Pd Concave Nanocubes. *Chem. - A Eur. J.* **25**, 16397–16404 (2019).

114. Smith, M. L. *et al.* Modified Tobacco mosaic virus particles as scaffolds for display of protein antigens for vaccine applications. *Virology* **348**, 475–488 (2006).

115. Lim, J. S et al. Quantitative study of Au(III) and Pd(II) ion biosorption on genetically engineered Tobacco mosaic virus. *J Colloid Interface Sci* 455-461 (2009).

VITA

Vindula Basnayake

Candidate for the Degree of

Master of Science

Thesis: SUSTAINABLE, GREEN, AND CONTINUOUS SYNTHESIS AND CHARACTERIZATION OF PALLADIUM NANORODS

Major Field: Chemical Engineering

Biographical:

Education:

Completed the requirements for the Master of Science in Chemical Engineering at Oklahoma State University, Stillwater, Oklahoma in May, 2021.

Completed the requirements for the Bachelor of Science in Chemical Engineering at Mississippi State University, Starkville, Mississippi in 2019.

Experience:

Undergraduate Researcher at Mississippi State University from May, 2017 to December, 2017.

Graduate Research Assistant at Oklahoma State University from August 2019 to present.

Publication:

K. Z. Lee, V. B. Pussepitiya, Y. Lee, S. Loesch-Fries, M. T. Harris, S. Hemmati, K. Solomon, "Engineering Tobacco Mosaic Virus and its Virus-Like-Particles for Synthesis of Biotemplated Nanomaterials", Biotechnol. J., 2000311, 2020.